# Longitudinal Control of Heavy Duty Vehicles: Experimental Evaluation

**Diana Yanakiev, Jennifer Eyre,
Ioannis Kanellakopoulos**

*University of California, Los Angeles*

The contents of this report reflect the views of the authors who are responsible
for the facts and the accuracy of the data presented herein. The contents do not
necessarily reflect the official views or policies of the State of California. This
report does not constitute a standard, specification, or regulation.

# Longitudinal Control of Heavy Duty Vehicles: Experimental Evaluation

Diana Yanakiev

Jennifer Eyre

Ioannis Kanellakopoulos

UCLA Electrical Engineering

Los Angeles, CA 90095-1594

ii

# Longitudinal Control of Heavy Duty Vehicles: Experimental Evaluation

Diana Yanakiev, Jennifer Eyre, and Ioannis Kanellakopoulos

## Abstract

This report describes the results of the first phase of the project, which was funded under MOU 293. These results consist of (i) improved modeling of air brakes for heavy trucks and buses, which accounts explicitly for nonlinearities and delays, and (ii) novel nonlinear algorithms for longitudinal control of commercial heavy vehicles without intervehicle communication. These algorithms use nonlinear spacing policies, backstepping control design, and aggressive prediction schemes to deal with the presence of significant delays and saturations in the fuel and brake actuators. As a result, their performance in the presence of delays is almost identical to the performance achieved in the absence of delays. This is the first class of algorithms which can deal with delays without relying on intervehicle communication, a property that was heretofore believed impossible to achieve. The significance of this result in terms of ITS deployment is that now we have removed one of the major obstacles to autonomous vehicle following for commercial heavy vehicles (CHVs). It also means that we can implement adaptive cruise control in trucks and buses that are not equipped with expensive brake-by-wire systems usually referred to as EBS (Electronic Brake Systems); this includes virtually every CHV on the road today, since EBS is only now starting to appear as an option on new trucks.

## Keywords

| | |
|---|---|
| Adaptive Cruise Control | Control Systems |
| Advanced Vehicle Control Systems | Intelligent Vehicle Highway Systems |
| Automated Highway Systems Control | Longitudinal Control |
| Autonomous Intelligent Cruise Control | Public Transit |
| Buses | Speed Control |
| Commercial Vehicle Operations | Trucking |
| Control Algorithms | Vehicle Follower Control |

# Executive Summary

This project is concerned with the experimental evaluation of longitudinal control algorithms for commercial heavy vehicles (CHVs), and for this purpose we are using a Class 8 truck which was provided free of charge until December 1999 by Freightliner Corporation. This report describes the results of the first phase of the project, which was funded under MOU 293. The project is currently continuing, funded under MOU 314.

One of the most critical obstacles in the automated operation of CHVs is the presence of significant delays in the fuel and brake actuators. These delays are especially important in longitudinal control of vehicle platoons which do not employ intervehicle communication, because their effect becomes cumulative as it propagates upstream, resulting in considerably degraded performance.

Until last year, there were only two ways one could deal with the actuator delay problem:

1. Use intervehicle communication with preview: if the leading vehicle transmits its desired speed profile to the followers a little bit ahead of time, then every vehicle can start the corresponding maneuver at the right moment, thus compensating for the presence of the delays.

2. Ensure that all the automated CHVs have brake-by-wire capabilities, often referred to as Electronic Brake Systems (EBS). These systems transmit brake commands via electronic signals instead of the usual air pressure signals which are transmitted through the brake lines, thus resulting in a very significant reduction of the brake actuator delays, which are usually much more severe than fuel actuator delays.

Clearly , both of these solutions have some drawbacks. Intervehicle communication comes at a considerable additional cost of installation and maintenance, and it assumes that the other vehicles will be equipped with it as well. EBS systems are even more expensive; they are only now starting to appear as an OEM option on new trucks, so existing CHVs would have to be retrofitted with them, a process which further increases the associated cost.

Therefore, in this project (and the companion project 240), we first set out to find an alternative solution to the actuator delay problem. First, using data provided by AlliedSignal Truck Brake Systems, we developed more detailed models of air brakes for heavy trucks and buses, which account explicitly for nonlinearities and delays. Then, we designed novel nonlinear algorithms for longitudinal control of CHVs without intervehicle communication. We used two different approaches which are tailored to different performance requirements and computational resources. First, we designed algorithms that use nonlinear spacing policies, backstepping control design, and aggressive prediction schemes; their performance in the presence of large delays is almost identical to the performance achieved when the delays are negligible. This is the first class of algorithms which can deal with delays without relying on intervehicle communication, a property that was heretofore believed impossible to achieve. However, this desirable property comes at the expense of significant additional controller complexity. Therefore, we also designed much simpler PID-like controllers which use nonlinear spacing policies and a filtered estimate of the preceding vehicle's acceleration; their performance is only slightly lower than that of the backstepping-predictive schemes, but their computational requirements are much lower.

The significance of these results in terms of ITS deployment is that now we have removed one of the major obstacles to autonomous vehicle following for CHVs. It also means that we can implement adaptive cruise control in trucks and buses that are not equipped with EBS.

# Contents

# List of Figures

# 1 Introduction

Advanced Vehicle Control and Safety Systems (AVCSS) are an integral part of the rapidly growing national and international initiatives on Intelligent Transportation Systems (ITS) and Automated Highway Systems (AHS). These initiatives aim to significantly enhance safety and convenience, reduce emissions and fuel consumption, and increase traffic capacity of existing highways through vehicle and roadway automation. Among the more visible of the proposed automation scenarios is *platooning* (Hedrick et al. 1991, Ioannou and Xu 1994, Sheikholeslam and Desoer 1990, Shladover 1978, Varaiya 1993), in which vehicles travel at highway speeds in fully automated and tightly spaced groups.

While full automation is the long-term goal, AHS deployment is likely to proceed in incremental stages, utilizing available results as early as possible. In the first stage, for example, vehicles would have only longitudinal control capabilities for vehicle following without intervehicle communication, with the driver assuming responsibility for steering and emergency situations. In that respect, systems currently in various stages of research and development can be classified into three categories:

- **Autonomous systems** depend only on information obtained by the sensors located on the vehicle itself, usually relative distance and velocity to stationary objects and moving vehicles. They are therefore implementable in the immediate future, and in fact have started to appear as commercial products (collision warning, adaptive cruise control).

- **Cooperative systems** add information transmitted by neighboring vehicles, usually acceleration and steering inputs. Hence, they can perform more demanding tasks than autonomous systems, such as coordinated driving in a group, but their time to commercialization is likely to be longer.

- **Automated highway systems** add information obtained from the roadway infrastructure, such as messages regarding traffic conditions and road geometry, and lateral information from magnetic nails or reflective guardrails installed on the highway. Such systems can perform even more demanding tasks, like fully automated driving in a platoon, but must face many more obstacles (standardization, liability issues, public acceptance) on their way to implementation.

It is worth noting that commercial vehicles will benefit from automation in all intermediate stages, both in terms of safety and traffic throughput. Of course, the reverse is true as well: AHS research will benefit from advances made in the design of heavy vehicles. In fact, the problem of slow brake response is already being addressed in the commercial trucking industry, albeit for safety reasons rather than as a consideration for AHS. CHV manufacturers are beginning to equip their vehicles with brake-by-wire systems, commonly referred to as Electronic Braking Systems (EBS), which significantly reduce brake actuator delays in order to meet ever-stricter government regulations on braking distances. While these developments justify our efforts on controller design for vehicles with very small actuator delays (Yanakiev and Kanellakopoulos 1995, 1996, 1998)

briefly reviewed here in section 3.1, their widespread implementation is yet to come. Furthermore, one has to remember that EBS is even farther away when it comes to trailer brakes, where the largest delays occur. And even if we assume that all future trailers will be equipped with EBS, controller design must still allow for large delays: Since tractor/trailer combinations are mixed and matched, a tractor modified for automated operation must also be able to pull a trailer without EBS.

In light of these short-term objectives, it becomes imperative to design controllers which will require only minimal modifications to vehicles currently in operation and production. Our previous controller designs (Yanakiev and Kanellakopoulos 1995, 1996, 1998) were based on the fact that for the purpose of AHS participation, CHVs will be equipped with actuators which feature considerably reduced delays. In simulations where delays were assumed to be small, our adaptive nonlinear controllers and nonlinear spacing policies demonstrated robust behavior in demanding merge-and-brake inter-platoon maneuvers, in addition to the objective for which they were designed: maintaining small intra-platoon spacing errors. However, the nonlinear spacing policies which have proven so beneficial in vehicles with negligible actuator delays are not able to cope with the effects of large delays. Accounting for realistic air brake response delays has proven to be a formidable challenge for longitudinal control design in the vehicle following scenario.

While we always use a detailed nonlinear vehicle model for simulations, the original controller design of section 3.1 was based on a simplified first-order representation of a truck. Our goal was to introduce only as much controller complexity as was necessary in order to meet the performance requirements, and to justify any increase in complexity with a corresponding performance improvement. Hence, these controllers were robust enough to deal with the large discrepancies between the simple model used for design and the detailed one used for simulation. Now that significant actuator delays are also included in the simulation model, we remove some of this discrepancy by using a second-order model which includes the actuator dynamics. Starting from our original controller and using a backstepping procedure, we derive a new control law which demonstrates significantly improved performance in the presence of large actuator delays.

A traditional approach for systems with known delays and available plant models is the use of prediction. While beneficiary to the performance of a single vehicle, a predictive approach was not expected to be able to compensate for the cumulative effect of the delay in a platoon under autonomous operation. Nevertheless, as shown in sections 3.3 and 3.4, the inclusion of an aggressive predictor in the control loop improves both the platoon performance and the control smoothness, thus enhancing safety and reducing fuel consumption.

The performance of the backstepping-based nonlinear controller with the predictor is almost as good in the presence of large delays as that of our original proportional-integral-quadratic (PIQ) controller in the delay-free case. However, this achievement comes at the expense of a significant increase in controller complexity and, hence, in its cost of implementation and installation. Therefore, in section 3.5, we propose a significantly simpler PID-like controller whose performance is actually better than the backstepping controller without the prediction. We hasten to stress, though, that this is not a PID controller, because it uses the nonlinear spacing terms of our original PIQ controller and has thus the same nonlinear complexity. While less complex than the backstepping-based scheme, this PID-based controller does not further improve its performance with the addition of predictive action.
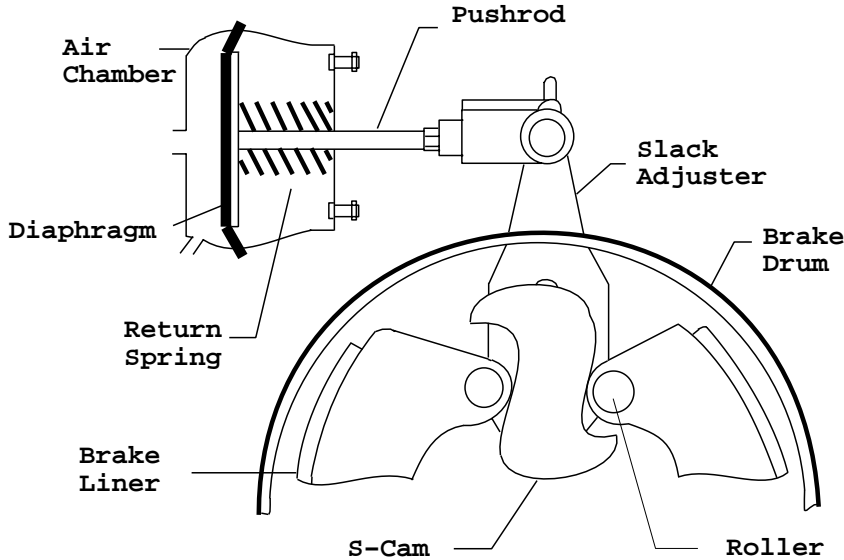
**Figure 1**: S-cam brake assembly.

# 2 Air Brake Modeling

In an effort to increase the accuracy of our simulations of platoons of automated commercial heavy vehicles (CHVs), we have undertaken to develop a model of CHV air brakes. This section describes the operation of a typical air brake system, and presents a SIMULINK brake model appropriate for inclusion in full vehicle simulations.

The braking system that is most prevalent in heavy-duty vehicles in North America is of the S-cam/drum variety (Leasure and Williams 1989), hence it is this brake assembly we will be modeling. As shown in Fig. 1, this brake is operated by a pushrod, which is actuated by pressure through a diaphragm in an air chamber. The pushrod is connected to a "slack adjuster", which is responsible both for converting the pushrod force into cam rotation and for the adjustment of the brakes (the length of pushrod stroke required for the linings to contact the drum). As the S-cam rotates, it forces the brake shoes out against the drum through rollers.

## 2.1 Pneumatic actuation

For longitudinal control purposes, the issue of interest is how quickly the brakes can respond to a control input. The air delivery system ("plumbing") has a significant impact on the speed of brake actuation, so an overview of its operation is included here.

Compressed air is stored in reservoirs on the tractor and trailer, and is fed to the brake chambers upon activation of the treadle (foot) valve. The front brakes receive air fairly quickly because of their proximity to the treadle valve and supply reservoir. The trailer brakes, however, must wait for an air pressure control signal to travel down a line from the tractor to the trailer. This signal controls a valve which connects the trailer brakes to an air supply reservoir located on the trailer. The control line has a smaller diameter than the air supply lines to speed transmission of the control

signal to the trailer, but the distance it must travel still results in substantial delays. This description is somewhat oversimplified, but should give a feel for why the trailer brakes are so slow to become active.

The time delay, measured from the initial activation of the treadle valve until the desired pressure is achieved at the brake diaphragm, can be broken into several components (University of Michigan seminar notes, Cogan 1983). The first is the brake response time, during which there is no detectable pressure in the air chamber. The chamber pressure then increases fairly linearly for a brief period as it fills with air, after which there is a rise time effect as the pressure is further increased to its desired value. This dynamic behavior is modeled as a pure time delay followed by a first order lag whose time constant is determined by the region of operation of the brake.

The pure time delay associated with the brake response depends on the location of the brake. Typical values for trailer brake delays are on the order of 200 ms. The front axle on the tractor, by comparison, has a delay of approximately 60 ms. In general, trailer brakes are the limiting factor in brake timing and control.

Three different time constants are used to completely characterize the behavior of the air pressure once it has reached the brake chamber. During the period when the chamber is being filled with air (typically until the pressure reaches approximately 10 psi) the time constant is assigned the relatively large value of .8 second to match the roughly linear increase shown by experimental data. Once the chamber has been filled, the time constant is decreased to a value of .14 second. This time constant is used during the entire apply region of operation, i.e., during the period that the pressure is increasing in the chamber. The time constant used during pressure decrease is slightly larger than that used during pressure increase, because the air chambers are able to be filled more quickly than they can be emptied. Hence, in the release region of operation the time constant is assigned a value of .16 second. Fig. 2 illustrates the response of the air pressure in the brake chamber to an input pressure at the treadle valve.

## 2.2 Torque generation

An analysis of forces acting on the brake shoes results in the following equation for calculating brake torque

$$T_{\mathrm{b}} = \frac{F_{\mathrm{p}} \, l \, S \, \mu \, R_{\mathrm{d}}}{R_{\mathrm{c}}} \tag{2.1}$$

where $F_{\mathrm{p}}$ is the pushrod force, $l$ is the slack adjuster length, $S$ is the shoe factor, $\mu$ is the lining/drum coefficient of friction, $R_{\mathrm{d}}$ is the drum radius, and $R_{\mathrm{c}}$ is the effective cam radius. For moderate braking, we will assume that the cam radius does not vary significantly, and will use its nominal value of .5 inch. The shoe factor is typically 2. The lining/drum friction coefficient is not constant; it is affected by a variety of factors that are very difficult to quantify, such as changes in brake temperature and work history. In addition, this coefficient varies from brake to brake of the same type by 20–30% (Post et al. 1975) and is therefore a highly uncertain quantity even before inclusion of other influences. Hence, we will use the relatively low value of $0.35$ for simulation as recommended by Heusser (1991) and neglect the effects of temperature and work history. The slack arm length and drum radius can be measured or are given, leaving only the calculation of pushrod force.
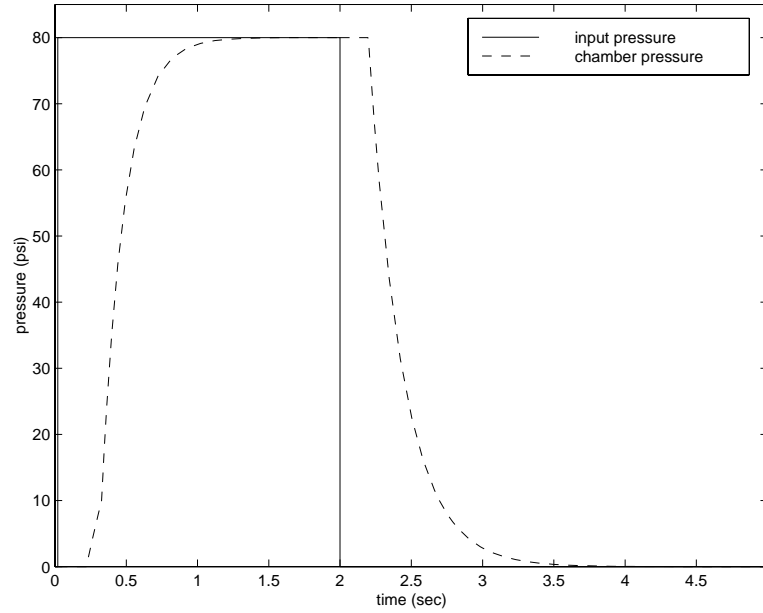
**Figure 2**: Pneumatic timing of trailer brake (simulation).

In the ideal case, the pushrod force can be determined using the relationship

$$F_\text{p} = P\,A \tag{2.2}$$

where $P$ is the pressure at the diaphragm and $A$ is the air chamber area. This is a reasonable approximation over certain ranges of air pressure and pushrod stroke. For low pressures and at long stroke, however, the force generated is not accurately represented by this relationship. If we assume that the brakes are in proper adjustment and are applied for brief durations, the pushrod stroke can be assumed to stay within the range for which the approximation is valid. The same assumption cannot be made for the applied pressure, because the pressure will frequently be in the low to moderate range for AHS applications. Therefore, a more accurate translation of pressure to pushrod force is desirable.

Using charts generated by Rockwell International (Heusser 1991), which list pushrod force as a function of stroke and pressure for a given air chamber size, an equation for calculating the pushrod force as a function of the chamber pressure was developed:

$$F_\text{p} = 29.222\,P - 112.2\,. \tag{2.3}$$

This equation is valid for a Type 30 (30 in$^2$) air chamber, for pressures between 10 psi and 90 psi, and for pushrod strokes between .5 inch and 1.875 inches (the range over which this brake is considered to be properly adjusted). Similar equations can be derived to calculate the pushrod force for other chamber sizes.

An initial minimum pressure, referred to as the "push-out pressure", must be achieved before any braking torque is generated. This is the pressure required to push the brake pads out against the drum, and it introduces an additional dead zone into the brake response. To simulate this effect, the
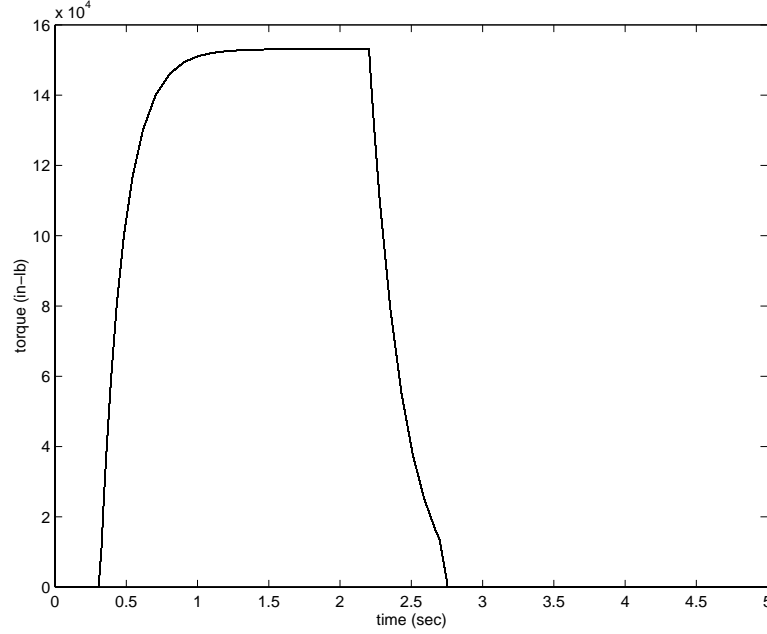
**Figure 3**: Torque response for typical trailer brake (simulation).

actuation force is set to zero for pressures below the push-out pressure. For the brakes considered here, the push-out pressure is typically in the range of 4–8 psi. A linear interpolation between the push-out pressure and 10 psi is used to calculate the pushrod force in this region. Therefore, the complete description of the conversion of air pressure to pushrod force is given by

$$
F_{\mathrm{p}} = \begin{cases} 29.222P - 112.2 & 10 \text{ psi} \leq P \\ \frac{180}{10-P_{\mathrm{po}}}P - \frac{180}{10-P_{\mathrm{po}}}P_{\mathrm{po}} & P_{\mathrm{po}} \leq P < 10 \text{ psi} \\ 0 & P \leq P_{\mathrm{po}} \end{cases} \tag{2.4}
$$

where $P_{\mathrm{po}}$ is the push-out pressure. Fig. 3 plots the torque response of a trailer brake to the pulse pressure input shown in Fig. 2.

Experimental data indicates that S-cam brakes exhibit pronounced hysteresis when applied at low vehicle velocities. These effects are much less apparent when the vehicle is traveling at highway speeds. To simulate this behavior, the brake model includes a backlash block whose dead-band width is determined by the initial vehicle velocity. At chamber pressures below the push-out pressure, the torque output is forced down to zero to avoid the offset inherent in the backlash block. Figs. 4 and 5 illustrate the torque output generated by the same pressure input for two different initial velocities.

The dynamic model for a single air brake is not unlike those developed for automobile brakes; however, air brake systems exhibit several characteristics that are not seen in automobile brakes which have a significant impact on the overall braking response and on controller design.

In automobile brakes, the time delay and response times at each axle will not differ significantly. For heavy commercial vehicles, although the goal is to have a pneumatically timed braking system in which all brakes respond virtually simultaneously, in practice the application times for

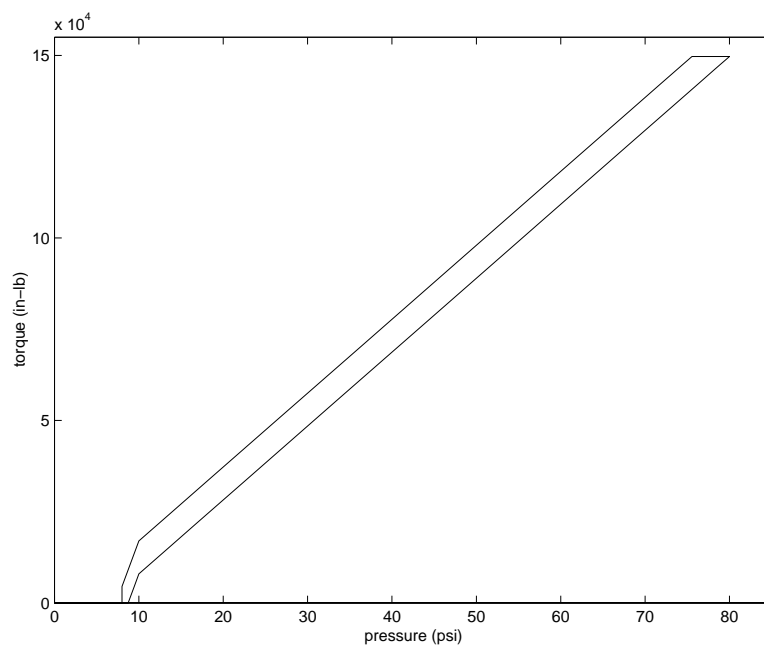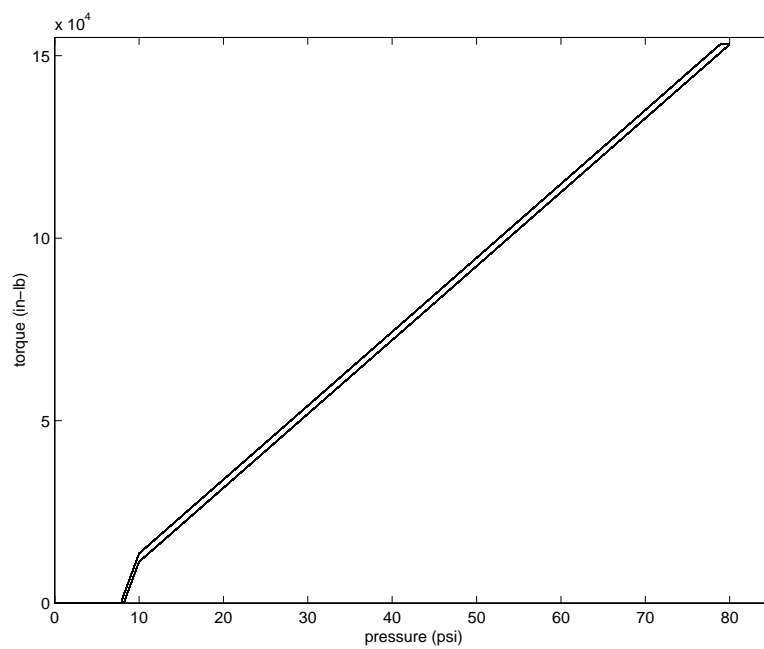**Figure 4**: Brake hysteresis at 2 mph (simulation).



**Figure 5**: Brake hysteresis at 40 mph (simulation).

different axles can vary significantly because of the differences in control line tube lengths (Radlinski and Flick 1986). To accurately represent the overall brake response, these timing differences will be included in the complete brake model.

Another factor that affects the performance of commercial vehicle braking systems is the variation in application pressures from brake to brake. Until sufficient pressure is generated to activate all the brakes, a subset of the braking system will be doing all of the work. This unbalanced operation, which is characteristic of low-pressure braking, has several undesirable effects. These include severe overheating and wear of those brakes which have lower application pressures and, if it is the tractor brakes doing all the work, high compressive coupling forces at the kingpin. From a controller design standpoint, this is an interesting phenomenon because it suggests that it may be better to "snub" the brakes (repeatedly apply high pressure pulses) than "drag" the brakes (apply a constant low pressure), especially on downgrades.

The sluggish response that is characteristic of air brakes (particularly at the trailer axles) can be addressed through implementation of a brake-by-wire system, commonly referred to as EBS. In this system, the air control line is replaced by an electronic control signal, thus eliminating the associated transmission line delay. Tractor manufacturers are already using EBS on their latest models, so it could be argued that the brake model need not include the lengthy delays associated with conventional air brakes. The problem with this assumption, however, is that tractors and trailers are "mixed and matched" by fleet operators. The life cycle of a trailer is many decades in duration - much longer than that of the tractor. Even if all new tractors are equipped with EBS, many of the trailers that will be towed will be not be similarly equipped. It makes sense, therefore, to retain the large delays in the simulation model.

Brake performance in general is affected by several variables that are extremely difficult to model: thermal response, brake adjustment, lining wear, and work history. This is true of both automobile and CHV brakes. Because of the uncertainty in the relationship between the brake chamber pressure and the actual torque output of the brake, it would be desirable to feed back the torque rather than the pressure. There are torque sensors currently in existence (Hurtig et al. 1994) which may be adaptable for this purpose.

The specific tractor/trailer configuration used for simulation is a Class 8 18-wheeler. This vehicle has three axles on the tractor and two on the trailer. Each axle has two brake chambers, for a total of ten. The tractor front brakes are Type 20 with 5.5-inch slack adjusters and 15x4-inch drums. The tractor rear brakes have Type 30 chambers with 5.5-inch slack adjusters and 16.5x7-inch drums. Finally, the trailer rear brakes are the same as the tractor rear brakes but with 6-inch slack adjusters. The maximum total brake torque that can be generated (assuming a maximum line pressure of 80 psi) is roughly $1.35 \text{x} 10^6$ inch-pounds. The additional braking power afforded by engine retarders is not considered here, as they are only used on downgrades.

## 2.3   Future research

The brake model used here is reasonably accurate at pressures above 10 psi. Below that threshold, the behavior of the air in the chamber is very difficult to model because of compressibility effects. This problem can be addressed either by attempting to increase the accuracy of the model using fluid dynamics analysis, or by employing an actuation method in which the desired pressure is always much higher than 10 psi (for example, pulse width modulation). Some analysis on the
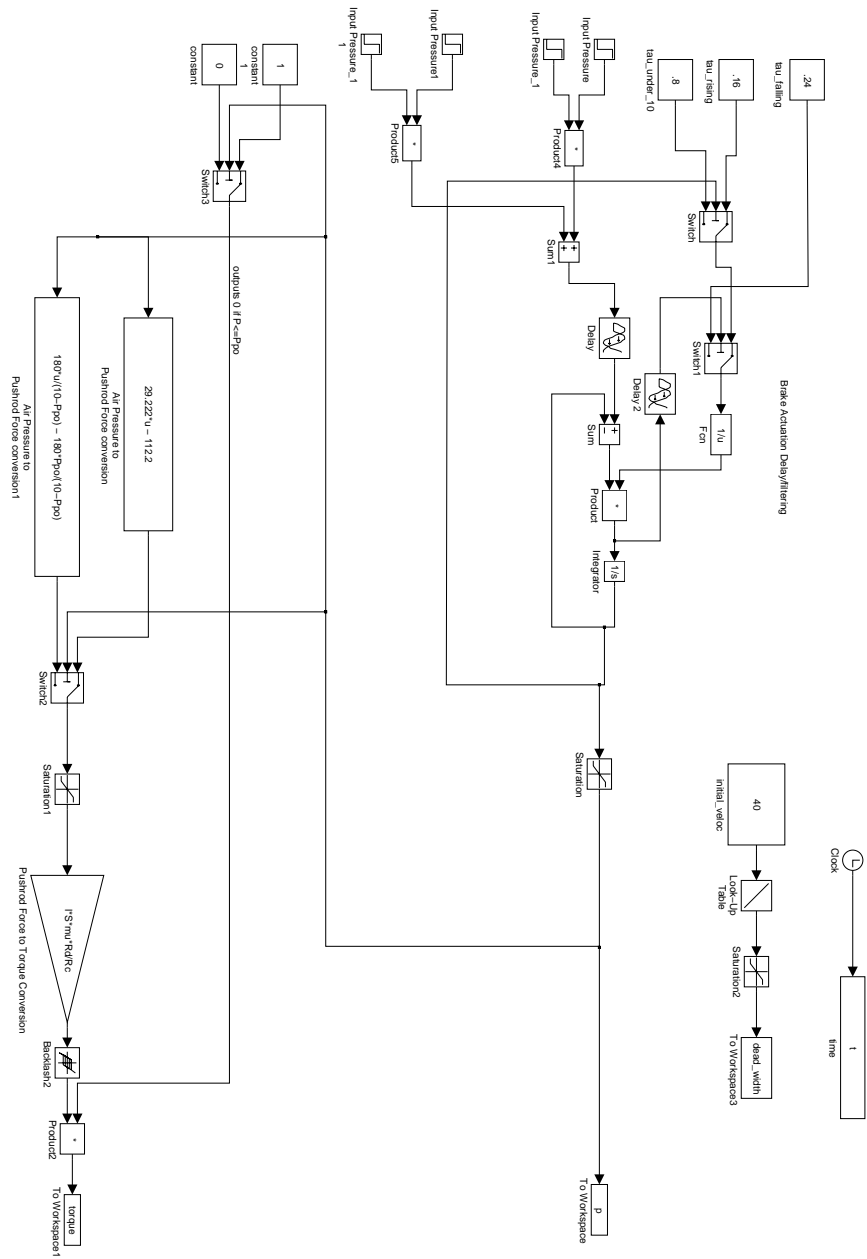
**Figure 6**: SIMULINK model of a single air brake.

tradeoffs and relative difficulty of each approach is needed.

The effects of temperature and rubbing speed between the brake pads and the drum have not been included, and provide a challenging area for model improvement.

# 3 Control with significant actuator delays

## 3.1 Adaptive PIQ controller

The parameters relevant to any two adjacent vehicles in a platoon are illustrated in Fig. 7. In
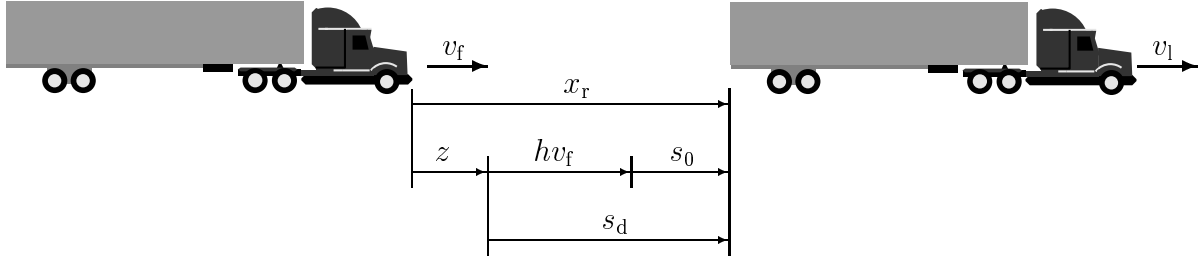


$$s_0 : \quad \text{minimum distance between vehicles}$$
$$h : \quad \text{time headway}$$
$$\text{(for speed-dependent spacing)}$$
$$x_r : \quad \text{vehicle separation}$$
$$s_d = s_0 + hv_f : \quad \text{desired vehicle separation}$$
$$v_l : \quad \text{velocity of leading vehicle}$$
$$v_f : \quad \text{velocity of following vehicle}$$
$$v_r = v_l - v_f : \quad \text{relative vehicle velocity}$$
$$z = x_r - s_d : \quad \text{spacing error}$$

**Figure 7**: Parameters for vehicle following.

the platoon scenario, the controller has to regulate to zero both the relative velocity $v_r$ and the separation error $\delta$,

$$v_r = v_l - v_f , \quad \delta = x_r - s_d , \tag{3.1}$$

where $v_l$ and $v_f$ are the velocities of the leading and following vehicle, while $x_r$ is the actual and $s_d$ the desired separation between vehicles. The desired separation may be constant (fixed spacing policy) or a function of the follower's velocity:

$$s_d = s_0 + hv_f \tag{3.2}$$

as shown in Fig. 7. The parameter $h$ is called *time headway* and its effect is to introduce more spacing at higher velocity in addition to the *constant spacing $s_0$*.

The tasks of regulating the relative velocity and the separation error can be combined into the control objective $v_r + k\delta = 0$, where $k$ is a positive design constant. This control objective makes

11

sense intuitively: If two vehicles are closer than desired ($\delta < 0$) but the leader's speed is larger than the follower's ($v_\mathrm{r} > 0$), then the controller in the follower does not need to take drastic action. The same can be said if the vehicles are farther apart than desired ($\delta > 0$) but the leader's speed is lower than the follower's ($v_\mathrm{r} < 0$). The selection of the coefficient $k$ influences the response of the controller, and can be changed depending on the performance requirements. In fact, as it has been shown by Yanakiev and Kanellakopoulos (1998), making this coefficient a nonlinear function of the separation error $\delta$ can significantly enhance platoon performance as well as control smoothness. We have also shown that when our control objective is achieved, i.e., when $v_\mathrm{r} + k\delta \equiv 0$, both the relative velocity and the separation error are regulated: $v_\mathrm{r} \to 0$ and $\delta \to 0$.

The adaptive PIQ developed by Yanakiev and Kanellakopoulos (1995, 1996)

$$u = \hat{k}_\mathrm{p}(v_\mathrm{r} + k\delta) + \hat{k}_\mathrm{i} + \hat{k}_\mathrm{q}(v_\mathrm{r} + k\delta)|v_\mathrm{r} + k\delta| \,, \tag{3.3}$$

is based on the linearized first-order vehicle model. The time-varying parameters $\hat{k}_\mathrm{p}$, $\hat{k}_\mathrm{i}$, and $\hat{k}_\mathrm{q}$ are being updated by an adaptive law.

The resulting adaptive PIQ controller can operate autonomously using a speed-dependent spacing policy. However, the fixed time headway has to be significantly larger than for passenger cars in order to guarantee good CHV platoon performance. In our previous work (Yanakiev and Kanellakopoulos 1995, 1998), we focus on the development of new nonlinear spacing policies which yield small separation errors without increased intervehicle spacing under autonomous vehicle operation. First, we introduce the notion of *variable time headway*: instead of being fixed, the headway varies with the relative speed $v_\mathrm{r}$ between adjacent vehicles as

$$h = h_0 - c_h v_\mathrm{r} \,, \tag{3.4}$$

where $h_0 > 0, c_h > 0$ are constant. The intuition behind this modification is as follows: Suppose that a vehicle wants to maintain a time headway of $h_0$ from the preceding vehicle, when both of them are traveling at the same speed. If the relative speed between the two vehicles is positive, that is, if the preceding vehicle is moving faster, then it is safe to reduce this headway, while if the preceding vehicle is moving slower then it would be advisable to increase the headway. The effect of introducing the variable time headway is quite dramatic: it results in an impressive reduction of errors and a considerably smoother control activity without any increase in steady-state intervehicle spacing.

Another modification is the introduction of a *variable separation error gain* $k$:

$$k = c_k + (k_0 - c_k)e^{-\sigma\delta^2} \,, \tag{3.5}$$

where $0 < c_k < k_0$ and $\sigma \geq 0$ are design constants. The intuition here is that when the separation error gain $k$ is constant, the controller will try to reduce a very large spacing error $\delta$ through a very large relative velocity $v_\mathrm{r}$ of opposite sign, in order to meet the desired control objective, which is $v_\mathrm{r} + k\delta = 0$. Hence, if a vehicle falls far behind the preceding vehicle, its controller will react aggressively by accelerating to a very high speed. This undesirable behavior can be corrected by decreasing the gain $k$ as $\delta$ becomes large and positive, making sure that it remains above some reasonable positive lower bound; this results in a smooth reduction of large spacing errors. The expression given in (3.5) does that, but also has another feature which at first glance may seem counter-intuitive: The gain $k$ is reduced even when $\delta$ becomes negative. This feature is

included due to the low actuation-to-weight ratio of CHVs, which severely limits the accelerations and decelerations they are capable of achieving. In autonomous operation, where each vehicle relies only on its own measurements of relative speed and distance from the preceding vehicle, aggressive control actions are amplified as they propagate upstream. Hence, during a sudden braking maneuver in a CHV platoon, only the first few vehicles will be able to achieve the necessary decelerations; the controllers of the next vehicles will quickly saturate, and collisions may occur. Reducing the gain $k$ for negative $\delta$ makes the reaction of the first few vehicles less aggressive and allows the remaining vehicles to follow safely, thus endows each vehicle's controller with a "group conscience", which sacrifices the individual performance of the first few vehicles in order to improve the overall behavior of the platoon.

## 3.2 Adaptive backstepping controller

The combination of the adaptive PIQ controller with the variable time headway and the variable separation error gain policies yields very good performance when the actuator delays are small, up to about $50$ ms. However, when we consider vehicles without EBS, the delays become significantly larger, in the order of $200$ ms. This makes the overall uncertainty (modeling errors and delays) too much for the above controller to handle. One possible approach to overcoming this problem would be to reduce the overall uncertainty by using a more accurate model for control design. For instance, we should account for the fact that the control input $u$ is not immediately present in the dominant (vehicle velocity) equation. Previously (Yanakiev and Kanellakopoulos 1998), we used a first-order model which resulted from linearization around the trajectory defined by $v_r + k\delta = 0$:

$$\dot{v}_f = a(v_r + k\delta) + bu + \bar{d}, \tag{3.6}$$

where $\bar{d}$ incorporates external disturbances and modeling errors, as well as the unknown nominal value of the control. Now we resort to a more elaborate model which is different from (3.6) in the following:

- it takes into consideration the presence of actuator dynamics; rather than assuming that the control input is directly present in (3.6), it recognizes the driving/braking torque $T$ as the input to (3.6) and adopts a first-order model to describe the actuator dynamics, i.e., the relationship between this torque and the actual control input $u$;

- it explicitly displays the aerodynamic drag in the vehicle velocity equation, rather than lumping it into the disturbance term $\bar{d}$; the aerodynamic drag term becomes significant at higher speeds and its inclusion in the control law yields better performance.

The new model then becomes:

$$\dot{v}_f = a(v_r + k\delta) + bT - \frac{C_a}{m}v_f^2 + d \tag{3.7}$$

$$\dot{T} = -a_1 T + a_1 u, \tag{3.8}$$

where $C_a$ is the aerodynamic drag coefficient, $m$ is the mass of the vehicle, and $d$ is the new disturbances term, which now excludes the effect of the drag.

Now we proceed in the following steps:

13

- First consider only (3.7). Determine the desired torque $T_d$ to regulate $v_r + k\delta$ as if $T$ were the actual control input in (3.7).

- Then, based on (3.8), we determine the actual control $u$ so that the difference between the desired and the actual torque converges to zero, i.e., $T - T_d \to 0$.

This procedure is based on the *backstepping technique* for nonlinear and adaptive control design, presented in detail in the recent book by Krstić et al. (1995).

We determine $T_d$ starting with our original design based on a first-order linearized model. Since now we want to explicitly account for the effect of the aerodynamic drag term, the desired torque becomes

$$T_d = u_{\text{orig}} + \frac{C_a}{bm} v_f^2 \,, \tag{3.9}$$

where $u_{\text{orig}} = u$ from (3.3). Then differentiating (3.9) and combining it with (3.8) yields:

$$\dot{T} - \dot{T}_d = -a_1 T + a_1 u - \dot{u}_{\text{orig}} - \frac{2C_a}{bm} v_f \dot{v}_f \,. \tag{3.10}$$

To ensure $T - T_d \to 0$, we augment the Lyapunov function that we use to derive the update laws for the adaptive controller parameters with the term $\frac{1}{2\gamma}(T - T_d)^2$

$$V_a = V + \frac{1}{2\gamma}(T - T_d)^2 \,, \tag{3.11}$$

where $\gamma > 0$ is a design constant. The time derivative becomes

$$\dot{V}_a = \dot{V} + \frac{1}{\gamma}(T - T_d)(\dot{T} - \dot{T}_d) \,. \tag{3.12}$$

Let $\beta$ be a positive design constant and define $c_1 = a_1\beta$. Adding and subtracting $c_1(T_d - T)$ to the right hand side of (3.10) and regrouping terms, we obtain

$$\dot{T} - \dot{T}_d = -c_1(T - T_d) - a_1(1 - \beta)T + a_1 u - \dot{T}_d - c_1 T_d. \tag{3.13}$$

Then (3.12) becomes

$$\dot{V}_a = \dot{V} - \frac{c_1}{\gamma}(T - T_d)^2 + \frac{1}{\gamma}(T - T_d)\left[-a_1(1 - \beta)T + a_1 u - \dot{T}_d - c_1 T_d\right] \,.$$

We should note that negative definiteness of $\dot{V}$ is no longer guaranteed, since $T$ and $T_d$ are different and an additional term appears in $\dot{V}$. Therefore, in order to guarantee negative definiteness of $\dot{V}_a$, hence asymptotic convergence of $T - T_d$ to zero, we need to choose $\gamma$ very small and we need the last term of (3.14) to vanish. The latter can be achieved with the control law

$$u = (1 - \beta)T + \frac{1}{a_1}\dot{T}_d + \beta T_d \,, \tag{3.14}$$

or

$$u = (1 - \beta)T + \frac{1}{a_1}\left(\dot{u}_{\text{orig}} + \frac{2C_a}{bm} v_f \dot{v}_f\right) + \beta\left(u_{\text{orig}} + \frac{C_a}{bm} v_f^2\right) \,.$$
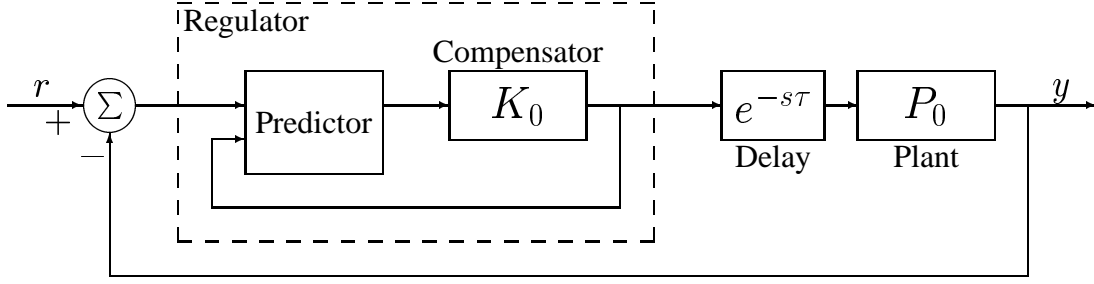
14

**Figure 8**: General predictor diagram.

This control law uses some quantities which were not needed in our previous designs. In particular, the acceleration of the current vehicle $\dot{v}_\text{f}$ is assumed to be measured, while the term $\dot{u}_\text{orig}$ contains the derivative of the error $\frac{d}{dt}(v_\text{r} + k\delta)$:

$$\dot{u}_\text{orig} = k_\text{p}\frac{d}{dt}(v_\text{r} + k\delta) + \gamma_\text{i}(v_\text{r} + k\delta) + k_\text{p}\frac{d}{dt}(v_\text{r} + k\delta)|v_\text{r} + k\delta|.$$

Of course, this derivative cannot be measured, since in autonomous operation we have no way of measuring the acceleration of the vehicle ahead. Here, we evaluate it using a so-called "dirty derivative", that is, an implementable approximation of the derivative operator, given by $\frac{s}{s\tau_\text{d}+1}$, where $\tau_\text{d}$ is small (as $\tau_\text{d} \to 0$, this operator becomes a pure derivative).

Tuning the design parameter to achieve good performance in our simulations, we realized that $\beta$ should be chosen small. Therefore, the complexity of the controller can be reduced by exclusion of the negligible terms and using the control law

$$u_\text{s} = T + \frac{1}{a_1}\left(\dot{u}_\text{orig} + \frac{2C_\text{a}}{bm}v_\text{f}\dot{v}_\text{f}\right) \tag{3.15}$$

instead of the one in (3.15).

## 3.3   Predictor design

A widely used approach for systems with known constant delays is to include a *predictor* in the control loop as shown in Fig. 8. One of the classic predictor structures is the *Smith predictor* (Smith 1957) shown in Fig. 9. The Smith predictor assumes that a compensator $K_0$ has already been designed for the plant $P_0$ to give a desired command response in the delay-free case. Then the compensator

$$K_\text{s} = \frac{K_0}{1 + (1 - e^{-s\tau})P_0K_0} \tag{3.16}$$

applied to the plant with the delay gives the same command response but with a delay of $\tau$ seconds. The main difficulty in our case is that we need to control a formation of several vehicles rather than just one individual truck, and we want to do this using a completely decentralized controller structure, with each vehicle depending only on its own measurements of the preceding vehicle's
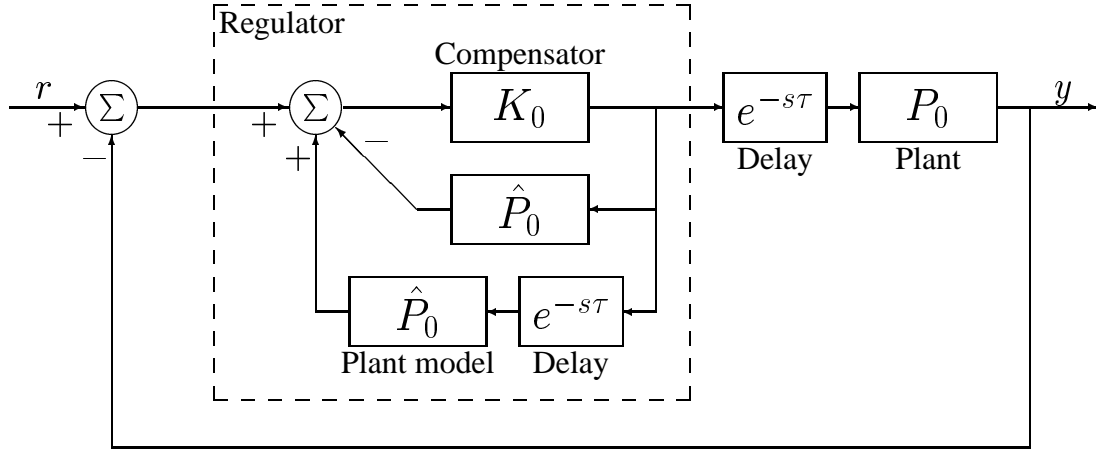
15

**Figure 9**: Smith predictor.

behavior. Therefore, delays in individual vehicle responses accumulate as they propagate upstream through the whole platoon. As a result, the stabilizing effect of the Smith predictor is limited only to the individual trucks and does not help much with the string stability of the whole platoon, since it cannot prevent the spacing and velocity errors from growing upstream. As expected, the Smith predictor applied to the original PIQ design based on the first-order linearized model could not achieve acceptable performance. Even when applied to the new control design presented in the previous section, the Smith predictor resulted in only slightly improved control smoothness. The latter is essential in automotive applications, where fuel consumption and passenger comfort and safety are important issues.

The fact that the Smith predictor does not fit our needs, however, does not mean that we should abandon the idea of using a predictor to compensate for delays. We have to look for a scheme which does not result in a delayed, albeit stable, response, but is truly predictive. The following reasoning was a starting point for our design. Suppose there is a delay of $\tau$ seconds from the issuing a control command until it is actually applied to the plant. If we were able to predict the state of the plant in $\tau$ s, we could issue a control command based on that estimate, $\hat{x}(t + \tau)$, rather than based on the current state of the plant, $x(t)$, which would no longer be appropriate when this control command reaches the plant in $\tau$ s. A first-order linear model is used to approximate the vehicle dynamics and to predict the spacing and velocity errors, $\delta$ and $v_{\mathrm{r}}$, respectively. A discrete representation with sampling period $\Delta$ is adopted for the implementation of the predictor. Let $\tau = l\Delta$, where $l$ is an integer. Hence, the state space representation of the above described predictor is

$$
\begin{aligned}
e_{i+l} &= a_{\mathrm{d}} e_{i+l-1} + b_{\mathrm{d}} u_{i-1} \\
e_{i+l-1} &= a_{\mathrm{d}} e_{i+l-2} + b_{\mathrm{d}} u_{i-2} \\
&\vdots \\
e_{i+1} &= a_{\mathrm{d}} e_i + b_{\mathrm{d}} u_{i-l}
\end{aligned}
\tag{3.17}
$$

where $e$ stands for "error" and represents either $v_{\mathrm{r}}$ or $\delta$, and $a_{\mathrm{d}}$ and $b_{\mathrm{d}}$ are the discretized parameters
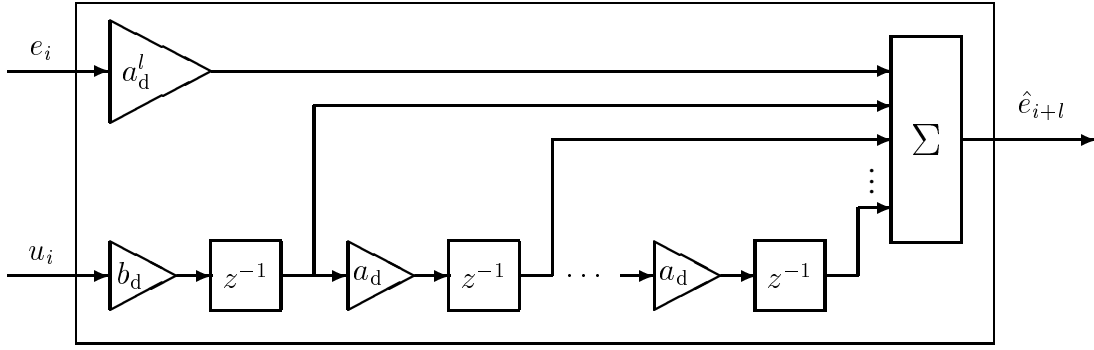
16

**Figure 10**: An alternative predictor with true predictive action.

$a$ and $b$ of the linear model $\frac{\delta v}{\delta u} = \frac{b}{s+a}$. This yields the predictor equation

$$e_{i+l} = a_{\mathrm{d}}^l e_i + a_{\mathrm{d}}^{l-1} b_{\mathrm{d}} u_{i-l} + a_{\mathrm{d}}^{l-2} b_{\mathrm{d}} u_{i-l+1} + \cdots + b_{\mathrm{d}} u_{i-1} . \tag{3.18}$$

The diagram in Fig. 10 illustrates the implementation of this scheme. Values of the control command from $u(t - \tau)$ to $u(t - \Delta)$ are stored in order to compute $\delta(t + \tau)$ and $v_{\mathrm{r}}(t + \tau)$ and based on them $u(t)$.

To investigate the stability properties of this scheme, we represent the whole system in discrete form, i.e., the delay $e^{-s\tau}$ becomes $z^{-l}$. The plant is denoted by $P_0 = \frac{\bar{b}_{\mathrm{d}}}{z - \bar{a}_{\mathrm{d}}}$, where the bars indicate that the model used in this predictor is not assumed to be accurate as in the case of the Smith predictor. Consider first the simplest case when $l = 1$ and the controller is just a proportional gain $K_0$. The transfer function of the regulator in Fig. 10 is

$$K_{\mathrm{r}} = \frac{K_0 a_{\mathrm{d}} z}{z - K_0 b_{\mathrm{d}}} . \tag{3.19}$$

The open-loop transfer function then becomes

$$H_{\mathrm{ol}}(z) = K_{\mathrm{r}} z^{-1} P_0 = \frac{K_0 a_{\mathrm{d}} \bar{b}_{\mathrm{d}}}{z^2 - (K_0 b_{\mathrm{d}} + \bar{a}_{\mathrm{d}})z + K_0 b_{\mathrm{d}} \bar{a}_{\mathrm{d}}} , \tag{3.20}$$

and the closed-loop transfer function of the system is

$$H_{\mathrm{cl}}(z) = \frac{\frac{K_0 a_{\mathrm{d}} \bar{b}_{\mathrm{d}}}{z(z - \bar{a}_{\mathrm{d}})}}{1 + K_0 (-b_{\mathrm{d}}) \frac{z - (\bar{b}_{\mathrm{d}} a_{\mathrm{d}}/b_{\mathrm{d}} + \bar{a}_{\mathrm{d}})}{z(z - \bar{a}_{\mathrm{d}})}} . \tag{3.21}$$

The closed-loop poles are

$$z_{1,2} = \frac{(K_0 b_{\mathrm{d}} + \bar{a}_{\mathrm{d}}) \pm \left[ (K_0 b_{\mathrm{d}} + \bar{a}_{\mathrm{d}})^2 - 4 K_0 (b_{\mathrm{d}} \bar{a}_{\mathrm{d}} + \bar{b}_{\mathrm{d}} a_{\mathrm{d}}) \right]^{\frac{1}{2}}}{2} . \tag{3.22}$$

Since $a_{\mathrm{d}} \approx \bar{a}_{\mathrm{d}}$ and $b_{\mathrm{d}} \approx \bar{b}_{\mathrm{d}}$, we can determine approximately the conditions for the closed-loop poles of the system to be inside the unit disk. It turns out that for $|z_{1,2}| < 1$ we need $0 < K_0 \bar{b}_{\mathrm{d}} <$
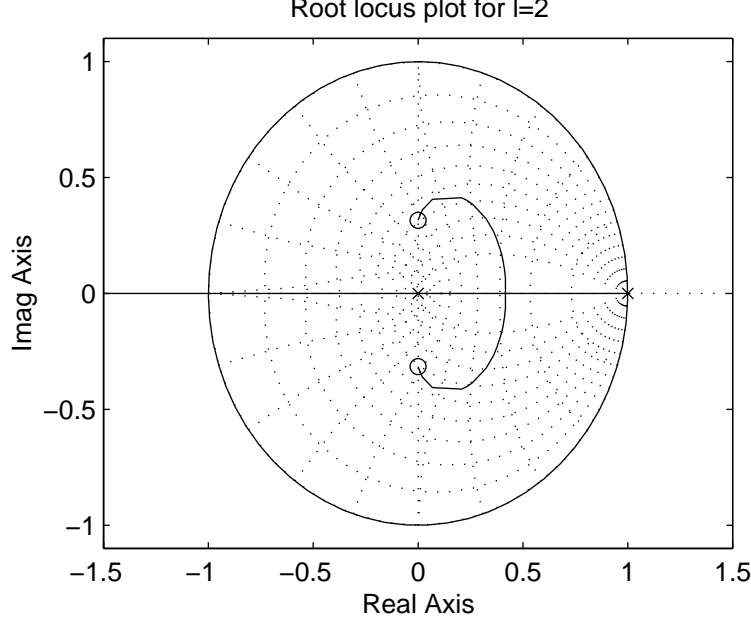
17

**Figure 11**: Root locus for $(-b_d) \dfrac{z^2 + (a_d - \bar{a}_d) z - a_d (\bar{b}_d a_d / b_d + \bar{a}_d)}{z^2 (z - \bar{a}_d)}$.

$\frac{1}{2\bar{a}_d}$. Since $\bar{a}_d \approx 1$ in our case, $K_0 \bar{b}_d < 0.5$ would guarantee stability of this scheme. However, if $b_d$ is negative in (3.21) and $b_d \approx -\bar{b}_d$, then $K_0 (b_d \bar{a}_d + \bar{a}_d b_d)$ cancels. Hence, one of the poles becomes approximately zero and the condition for the other one to be inside the unit disk is approximately $0 < K_0 \bar{b}_d < 2$, which is achievable for a wide range of $K_0$'s, since $\bar{b}_d$ is very small in our case.

Now consider the case when $l = 2$ and the controller is still just a proportional gain $K_0$. The transfer function of the regulator in Fig. 10 becomes

$$K_r = \frac{K_0 a_d^2 z^2}{z^2 - K_0 b_d z - K_0 a_d b_d} \ . \tag{3.23}$$

Hence, the closed-loop transfer function of the system is

$$H_{cl}(z) = \frac{\frac{K_0 a_d^2 \bar{b}_d}{z^2 (z - \bar{a}_d)}}{1 + K_0 (-b_d) \frac{z^2 + (a_d - \bar{a}_d) z - a_d (\bar{b}_d a_d / b_d + \bar{a}_d)}{z^2 (z - \bar{a}_d)}} \ . \tag{3.24}$$

Now we can plot the root locus of the open-loop transfer function which multiplies $K_0$ in the denominator of (3.24) and conclude that stability can be guaranteed for the same values of $K_0$ as in the $l = 1$ case. The root locus is shown in Fig. 11. It is worth noting that $b_d < 0$ again.

A more general result can be reached if we perform the calculations for an arbitrary value of $l$. Using the predictor equation (3.18), we obtain for the transfer function of the regulator in Fig. 10

$$K_r = \frac{K_0 a_d^l z^l}{z^l - K_0 b_d z^{l-1} - \cdots - K_0 a_d^{l-2} b_d z - K_0 a_d^{l-1} b_d} \ . \tag{3.25}$$

18

The closed-loop transfer function of the system is

$$
\frac{\frac{K_0 a_{\mathrm{d}}^l \bar{b}_{\mathrm{d}}}{z^l(z-\bar{a}_{\mathrm{d}})}}{1+K_0(-b_{\mathrm{d}})\frac{z^l+(a_{\mathrm{d}}-\bar{a}_{\mathrm{d}})z^{l-1}+\cdots+a_{\mathrm{d}}^{l-2}(a_{\mathrm{d}}-\bar{a}_{\mathrm{d}})z-a_{\mathrm{d}}^{l-1}(\bar{b}_{\mathrm{d}}a_{\mathrm{d}}/b_{\mathrm{d}}+\bar{a}_{\mathrm{d}})}{z^l(z-\bar{a}_{\mathrm{d}})}} . \tag{3.26}
$$

If the plant is modeled accurately, i.e., $a_{\mathrm{d}} = \bar{a}_{\mathrm{d}}$ and $b_{\mathrm{d}} = -\bar{b}_{\mathrm{d}}$, cancelation of terms will reduce the denominators of the transfer functions in (3.21), (3.24), and (3.26) to only

$$
1 + K_0 \frac{\bar{b}_{\mathrm{d}}}{z - \bar{a}_{\mathrm{d}}} = 1 + K_0 P_0 . \tag{3.27}
$$

Hence, the stability of the system with this predictor will be independent of the sampling, provided that the linear model used is an accurate representation of the plant.

## 3.4   Comparative simulations

To illustrate the capability of our control design to cope with the actuator delays, we use simulations of a platoon comprising seven (7) tractor-semitrailer combination vehicles. Both fuel and brake actuator have a pure time delay $\tau = 0.2\,\mathrm{s}$ each. The platoon starts out at an initial speed of $12\,\mathrm{m/s}$. At $t = 10\,\mathrm{s}$ the platoon leader is given a command to accelerate at $0.2\,\mathrm{m/s^2}$ for $10\,\mathrm{s}$. Then at $t = 35\,\mathrm{s}$ a command for deceleration at $3\,\mathrm{m/s^2}$ is issued for $3\,\mathrm{s}$. The minimum desired separation between vehicles is $s_0 = 3\,\mathrm{m}$. This demanding scenario is representative of the difficulties the system might have maintaining stable platoon behavior when trying to meet a challenging acceleration/deceleration objective. In all our simulation plots, different vehicles are represented by lines of different thickness: Vehicle 1 is shown with a thick solid line, while lines corresponding to the following vehicles become thinner as the vehicle's number in the platoon increases. The desired velocity profile is given in a dash-dotted line.

The original PIQ controller together with both nonlinear spacing policies, variable time headway $h = 0.1 - 0.2v_{\mathrm{r}}$ s and variable separation error gain $k = 0.1 + (1 - 0.1)e^{-0.1\delta^2}$ cannot yield acceptable performance because its gains have to be reduced in order to maintain stability in the presence of delays. Multiple crashes are observed in the "vehicle separation" plot of Fig. 12 due to the abrupt deceleration maneuver commanded from $t = 35\,\mathrm{s}$ to $t = 38\,\mathrm{s}$. The backstepping controller with the same nonlinear spacing policies achieves dramatic reduction of errors as it can be seen by comparing the plots of Fig. 14 to the ones of Fig. 12. The fact that the variable $h$ and $k$ still achieve superior performance is illustrated in Figs. 13 and 14, where the same backstepping controller is being used with constant and variable $h$ and $k$ respectively. However, the minor difference between Figs. 15 and 16 indicates that the role of these nonlinear spacing policies for performance enhancement is considerably diminished when the backstepping controller is used in the absence of significant actuator delays. Of course, when the original PIQ controller is used, variable $h$ and $k$ are necessary for acceptable performance even in the absence of delays as seen in Fig. 17. It is worth noting that while incapable to yield acceptable performance in the presence of significant delays, the PIQ design is tolerant to small actuator delays as seen in Fig. 18.

We also investigated the possibilities to achieve smoother control by adding a predictor to the control design. The results with the Smith predictor are shown in Fig. 19. The platoon performance is improved when the other predictor discussed in this section is used. The latter yields reduced

separation errors and smoother control as shown in Fig. 20. The backstepping design demonstrates reasonable robustness with respect to the value of the delay as seen in Figs. 21 and 22, where the value of the delay is increased to $\tau = 0.3\,\text{s}$. Comparison between these figures confirms the role of the alternative predictor as a smoothing factor for the control effort.

## 3.5   PID controller

As mentioned earlier, reducing controller complexity is essential for automotive applications where cost and simplicity of implementation are crucial. After reaching a solution to our longitudinal control problem in the absence of intervehicle communication, we would like to determine the key factor that renders the new design superior to the original one. Moreover, we can use that as a starting point to finding a simpler controller, which still provides the robustness with respect to actuator delays.

Originally we avoided the ubiquitous PID scheme because measurements of the derivative of the error are not available. Recall that only the relative distance and velocity with respect of the preceding vehicle, as well as the current vehicle velocity, are used by the controller. While it is realistic to obtain accurate measurements of the acceleration of the vehicle with nowadays technology, the preceding vehicle's acceleration cannot be measured directly. Therefore, a derivative term would not be physically implementable.

However, the backstepping design of section 3.2 results in a control law which also requires knowledge of the derivative of the error $\frac{d}{dt}\left(v_{\text{r}} + k\delta\right)$. There we substituted the derivative operator with its realizable approximation $\frac{s}{s\tau_{\text{d}}+1}$. Evaluation of the terms comprising the control law of (3.15) via computer simulations lead to the expected conclusion that the derivative action is crucial for achieving robustness with respect to delays. We can use the same approximation of the derivative term in the classical PID controller and obtain

$$u = k_{\text{p}}\left(v_{\text{r}} + k\delta\right) + k_{\text{i}}\frac{1}{s}\left(v_{\text{r}} + k\delta\right) + k_{\text{d}}\frac{s}{s\tau_{\text{d}}+1}\left(v_{\text{r}} + k\delta\right) \tag{3.28}$$

Under these circumstances, it is only natural to compare the performance of a PID controller to the controller in (3.15) and determine whether the complexity of the latter is justified by its performance. It turns out that without the nonlinear modifications of the control objective proposed in section 3.2, i.e., variable time headway, $h$, and variable separation error gain, $k$, the PID controller is incapable of achieving acceptable performance in the presence of actuator delays. However, if variable $h$ and $k$ are used, the performance of the PID scheme is similar and even better in certain aspects than the nonlinear design of section 5.1. One can verify this by comparing the PID controller results plotted in Fig. 23 to the backstepping scheme in Fig. 14 and even its version with the alternative predictor scheme in Fig. 20. Not only does the PID controller result in spacing errors of similar magnitude during the transient phase, but it also yields faster convergence of the errors to zero. One should keep in mind that the negative spacing errors are the most undesirable in the vehicle following scenario because they can result in collisions. Moreover, the PID scheme also demonstrates reasonable robustness with respect to the value of the delay. This is can be observed in Figs. 25 and 26 where $\tau = 0.3\,\text{s}$. The alternative predictor still improves control smoothness as seen by comparing Fig. 24 to Fig. 23 and Fig. 26 to Fig. 25.
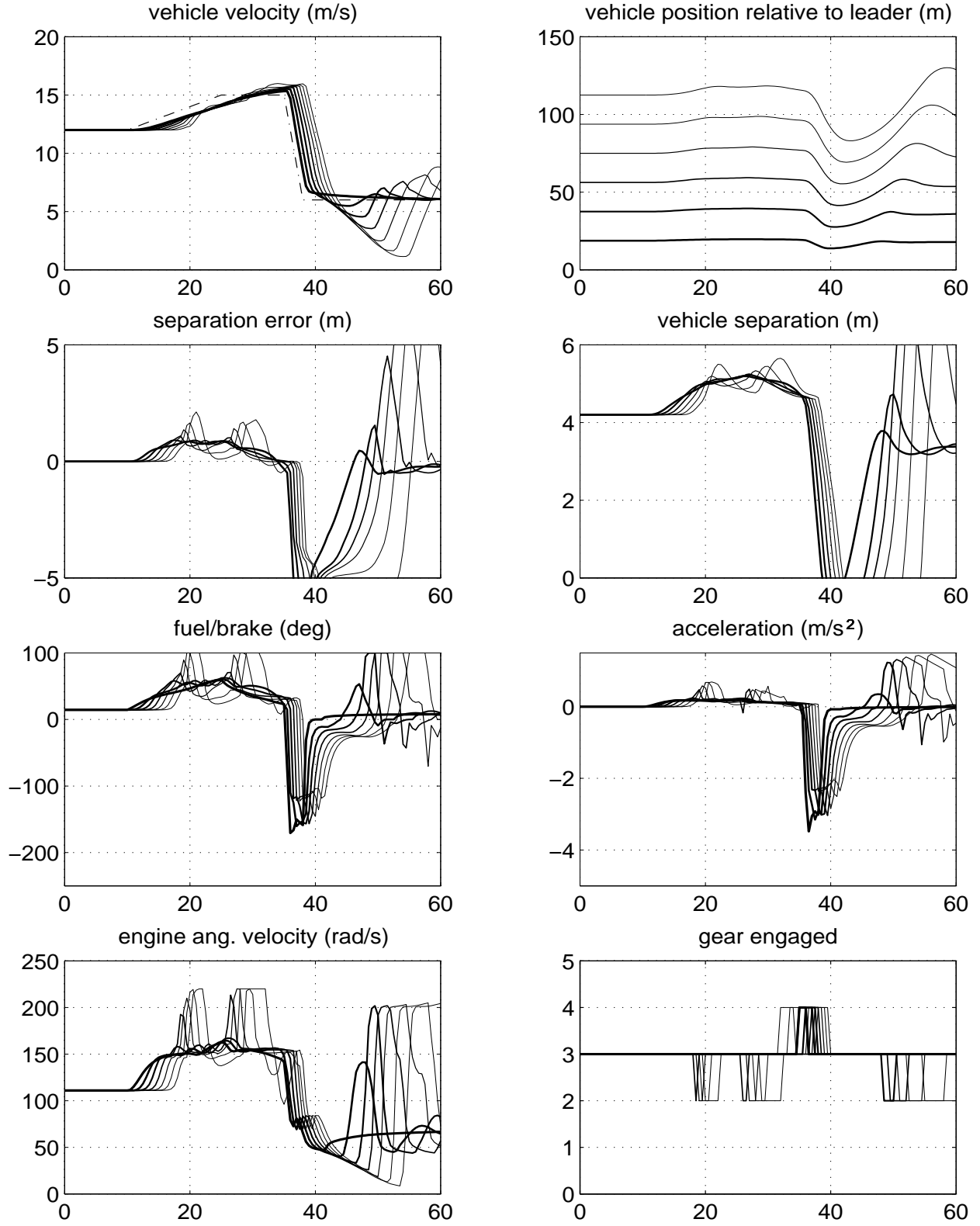
20

**Figure 12**: Actuator delay $\tau = 0.2$ s, original PIQ controller with variable time headway $h = 0.1 - 0.2v_{\mathrm{r}}$ s and variable separation error gain $k = 0.1 + (1 - 0.1)e^{-0.1\delta^2}$.
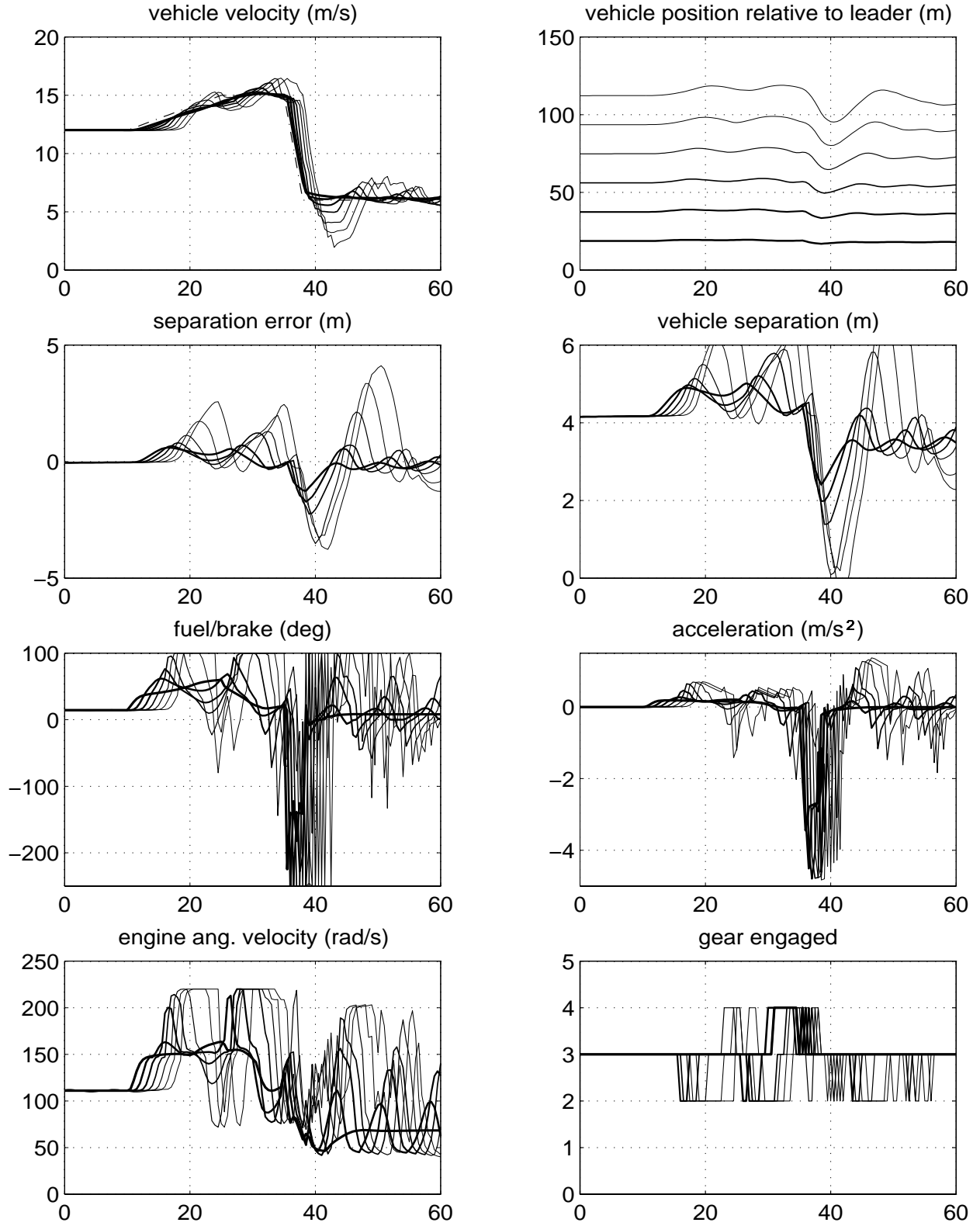
21

**Figure 13**: Actuator delay $\tau = 0.2$ s, backstepping controller with constant time headway $h = 0.1$ s and constant separation error gain $k = 1$.
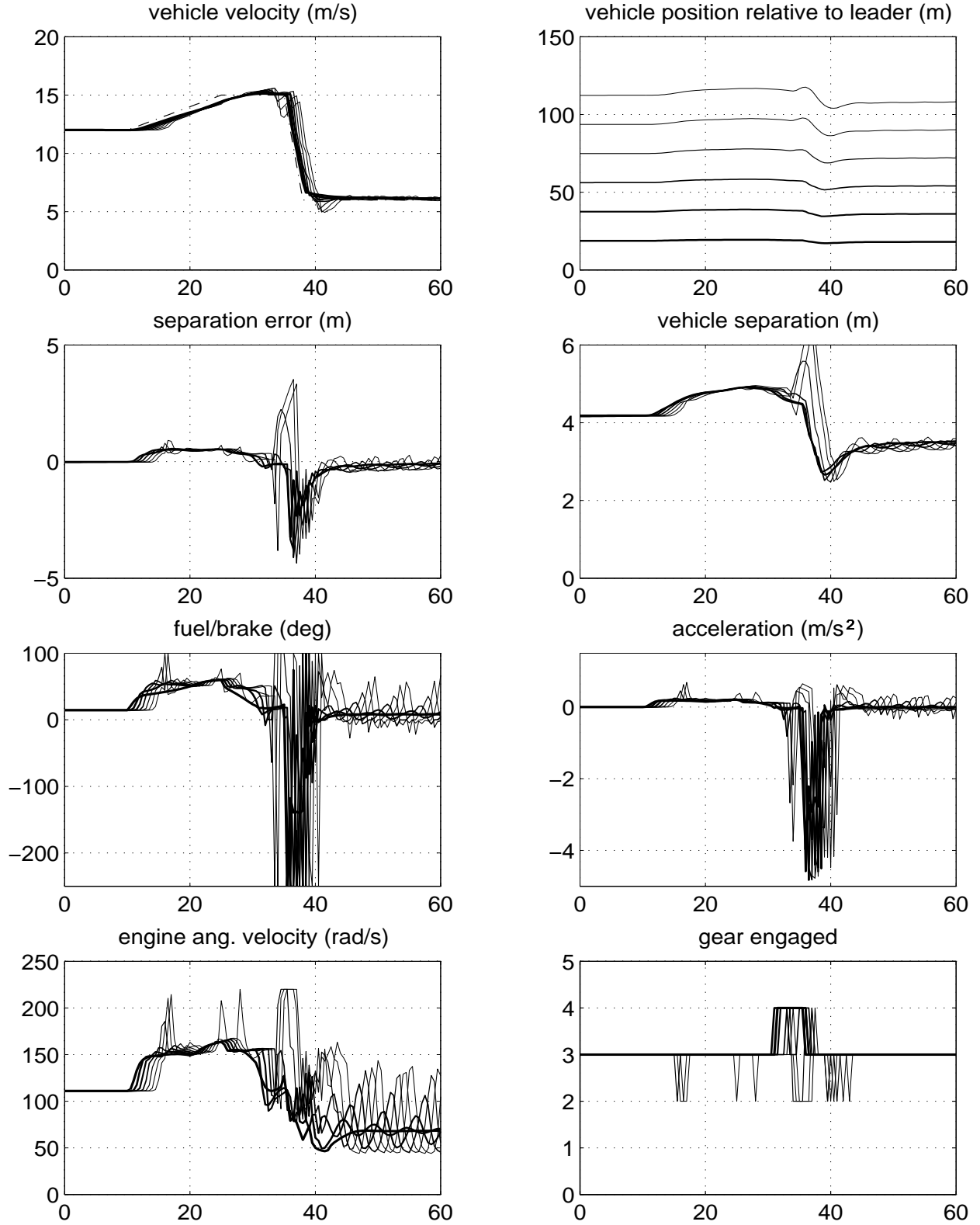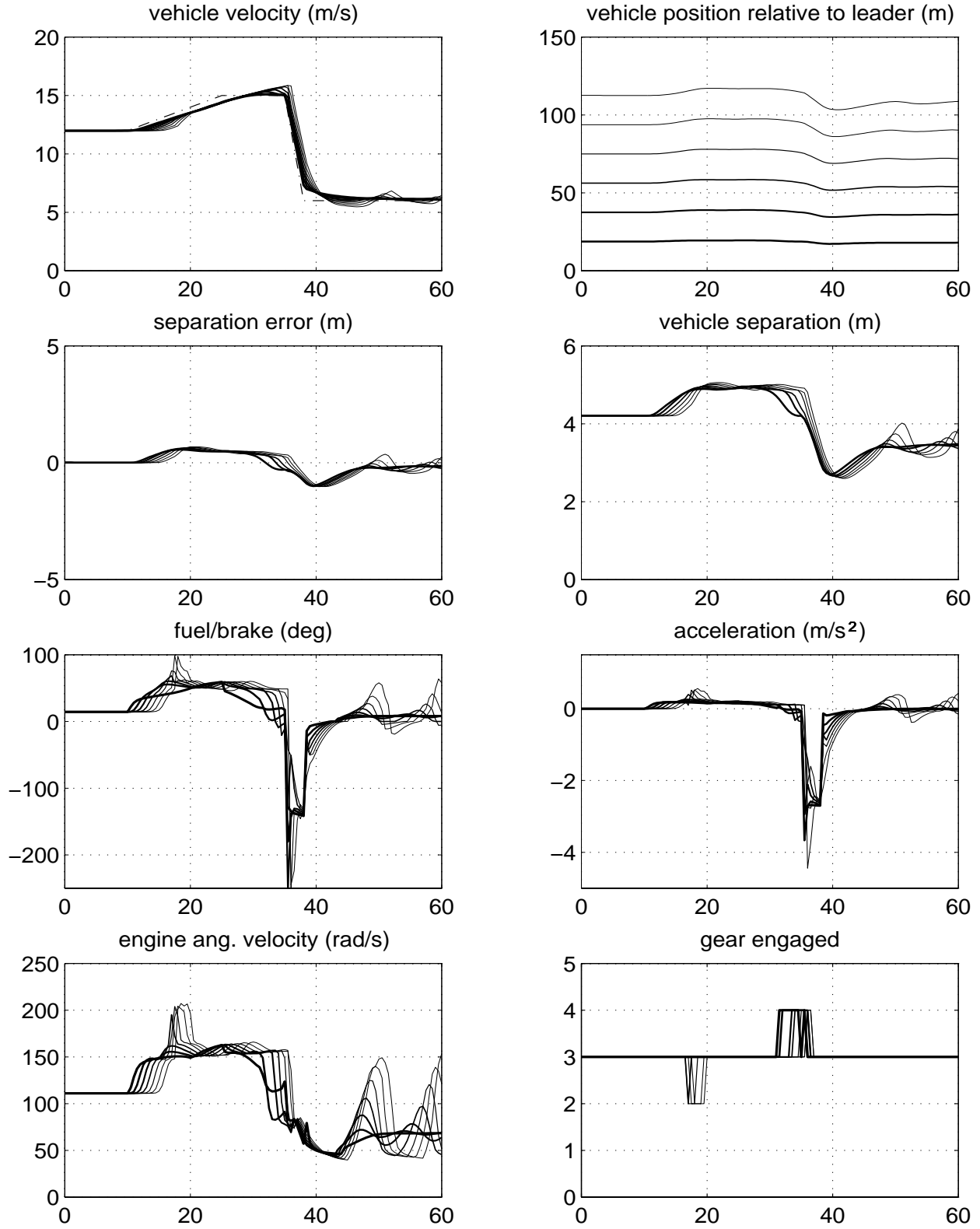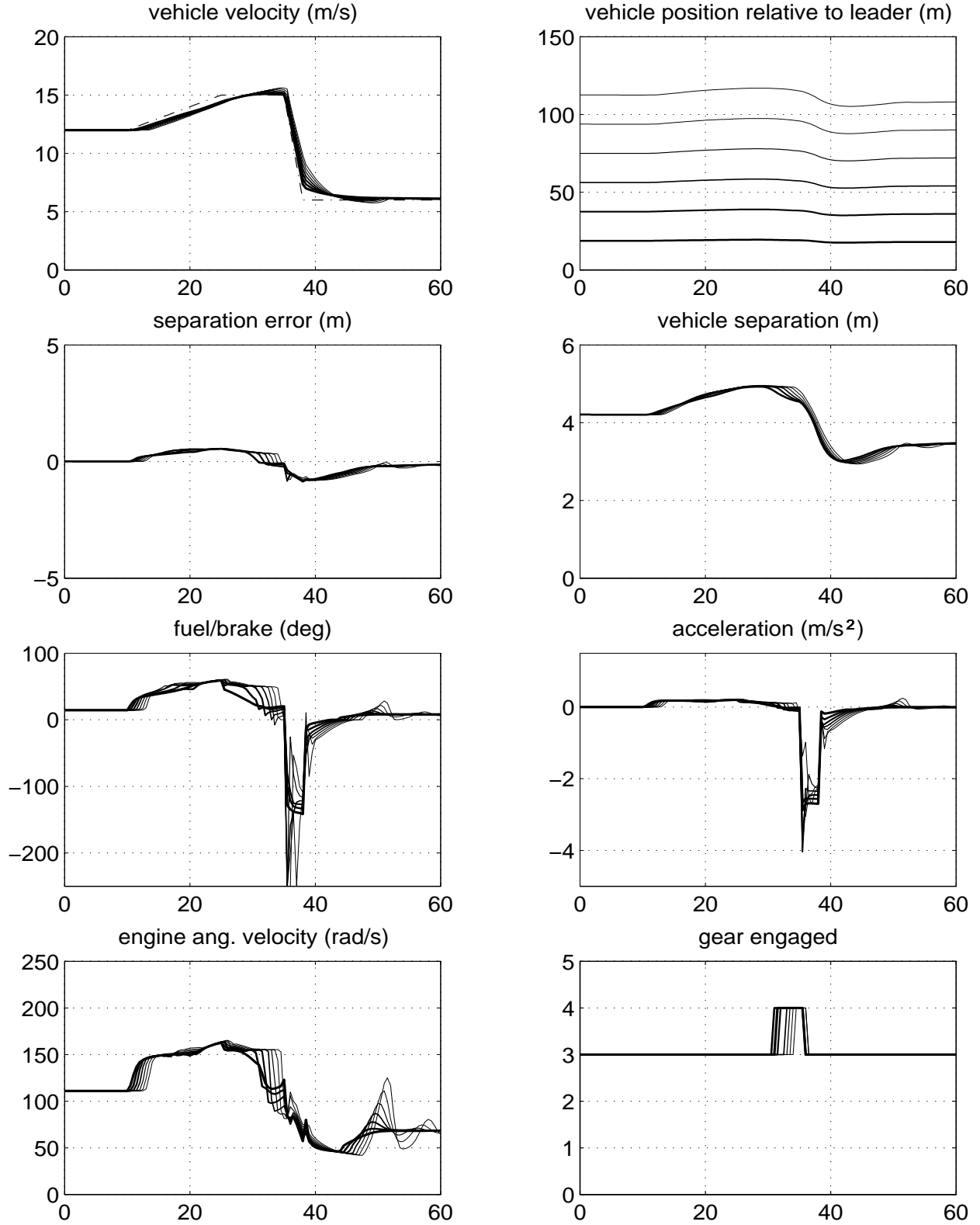
22

**Figure 14**: Actuator delay $\tau = 0.2$ s, backstepping controller with variable time headway $h = 0.1 - 0.2v_{\mathrm{r}}$ s and variable separation error gain $k = 0.1 + (1 - 0.1)e^{-0.1\delta^2}$.
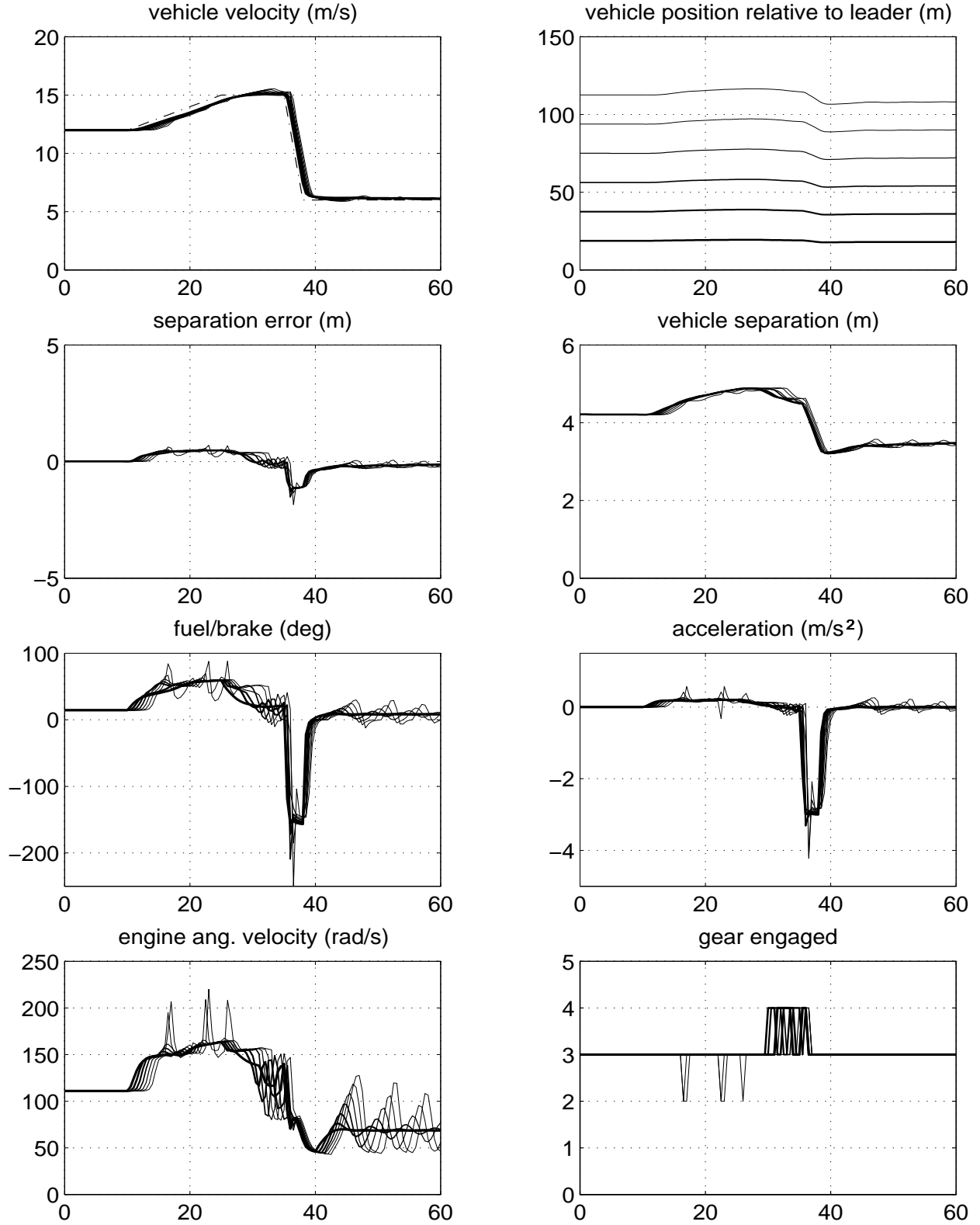
**Figure 15**: No delay, backstepping controller with constant time headway $h = 0.1$ s and constant separation error gain $k = 1$.

24

**Figure 16**: No delay, backstepping controller with variable time headway $h = 0.1 - 0.2v_r$ s and variable separation error gain $k = 0.1 + (1 - 0.1)e^{-0.1\delta^2}$.
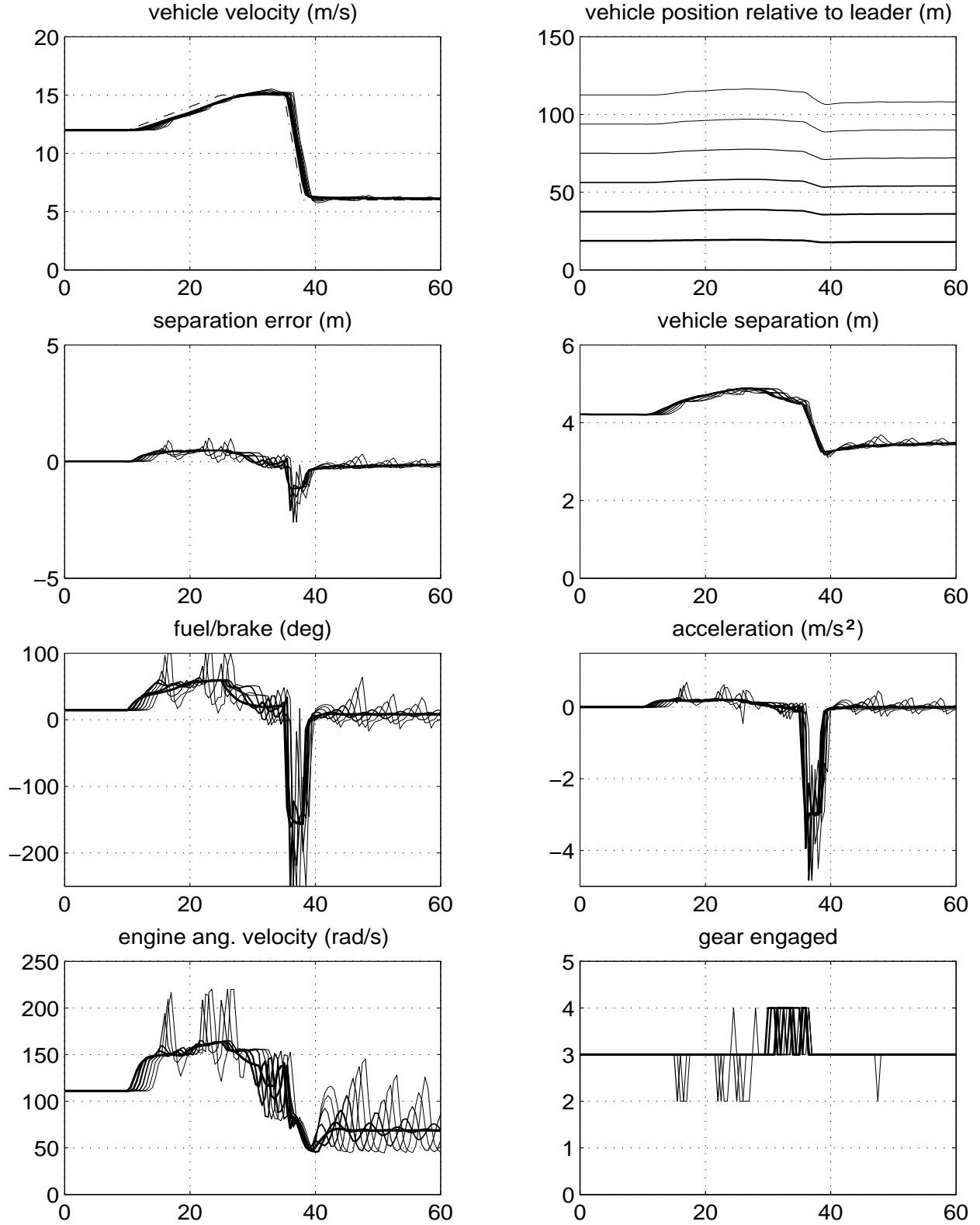
25

**Figure 17**: No delay, original PIQ controller with variable time headway $h = 0.1 - 0.2v_r$ s and variable separation error gain $k = 0.1 + (1 - 0.1)e^{-0.1\delta^2}$.

**Figure 18**: Actuator delay $\tau = 0.05$ s, original PIQ controller with variable time headway $h = 0.1 - 0.2v_r$ s and variable separation error gain $k = 0.1 + (1 - 0.1)e^{-0.1\delta^2}$.
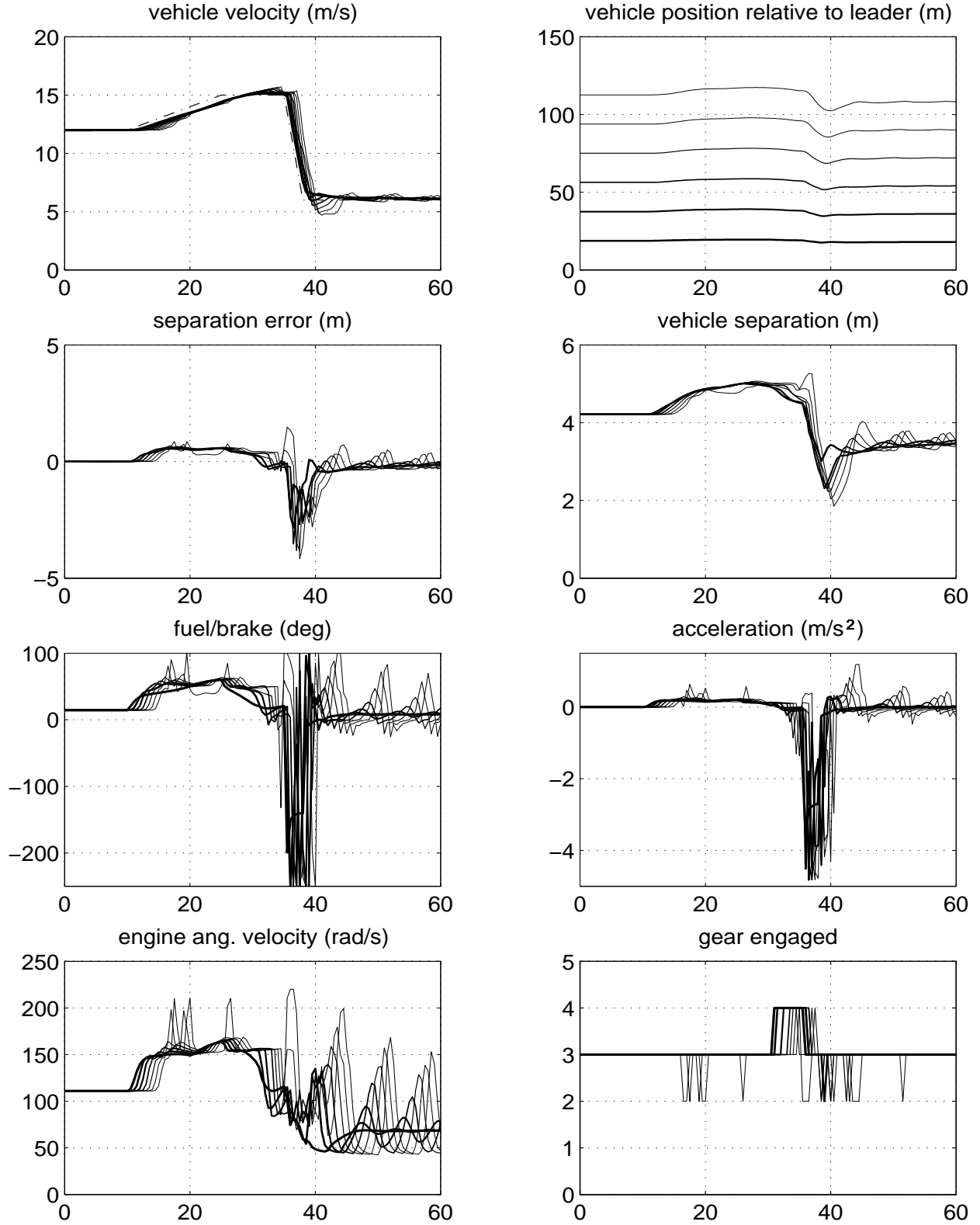
**Figure 19**: Actuator delay $\tau = 0.2$ s, backstepping controller with Smith predictor variable time headway $h = 0.1 - 0.2v_{\mathrm{r}}$ s, and variable separation error gain $k = 0.1 + (1 - 0.1)e^{-0.1\delta^2}$.
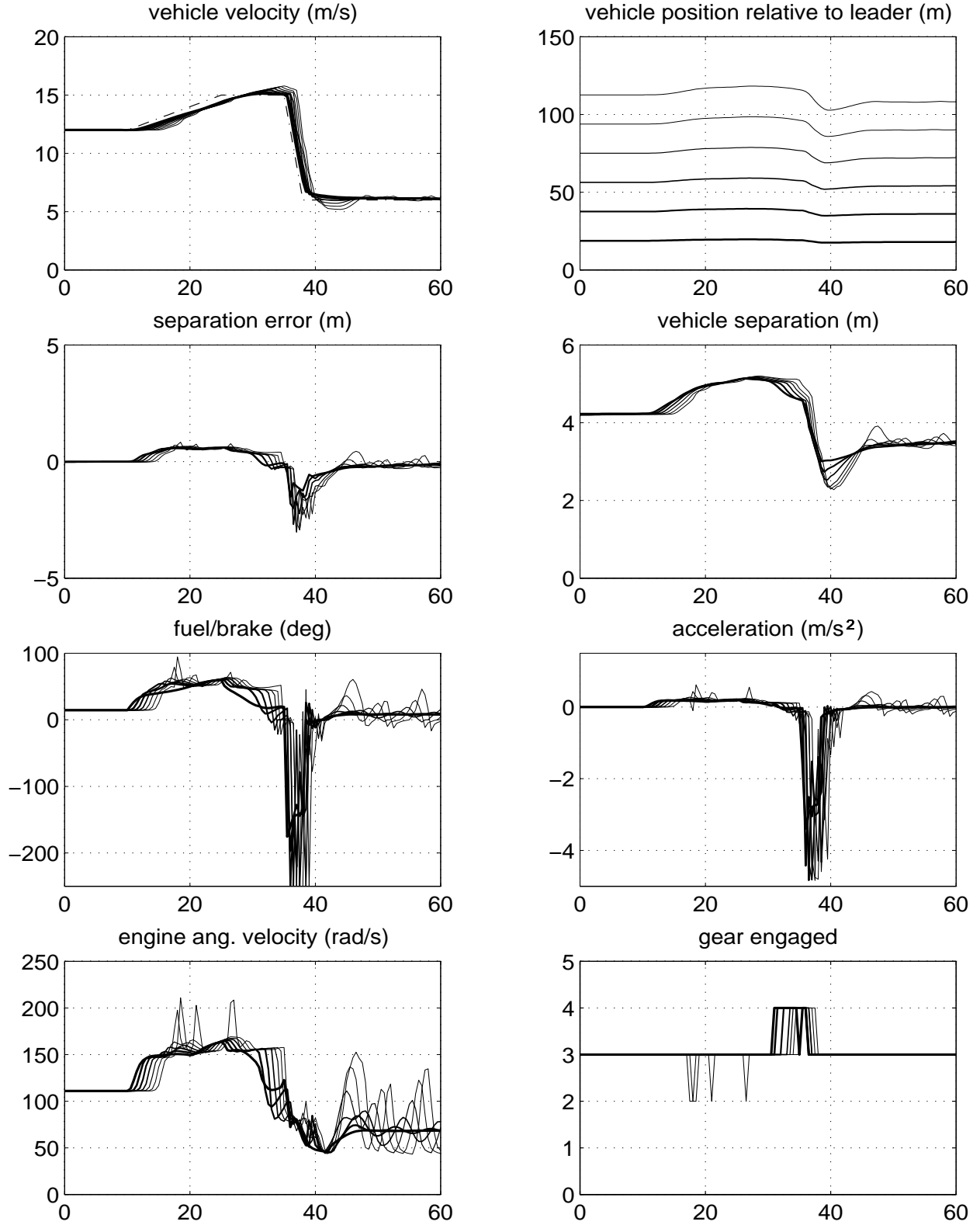
**Figure 20**: Actuator delay $\tau = 0.2$ s, backstepping controller with alternative predictor, $l = 5$, $\Delta = 0.04s$, variable time headway $h = 0.1 - 0.2v_{\mathrm{r}}$ s, and variable separation error gain $k = 0.1 + (1 - 0.1)e^{-0.1\delta^2}$.
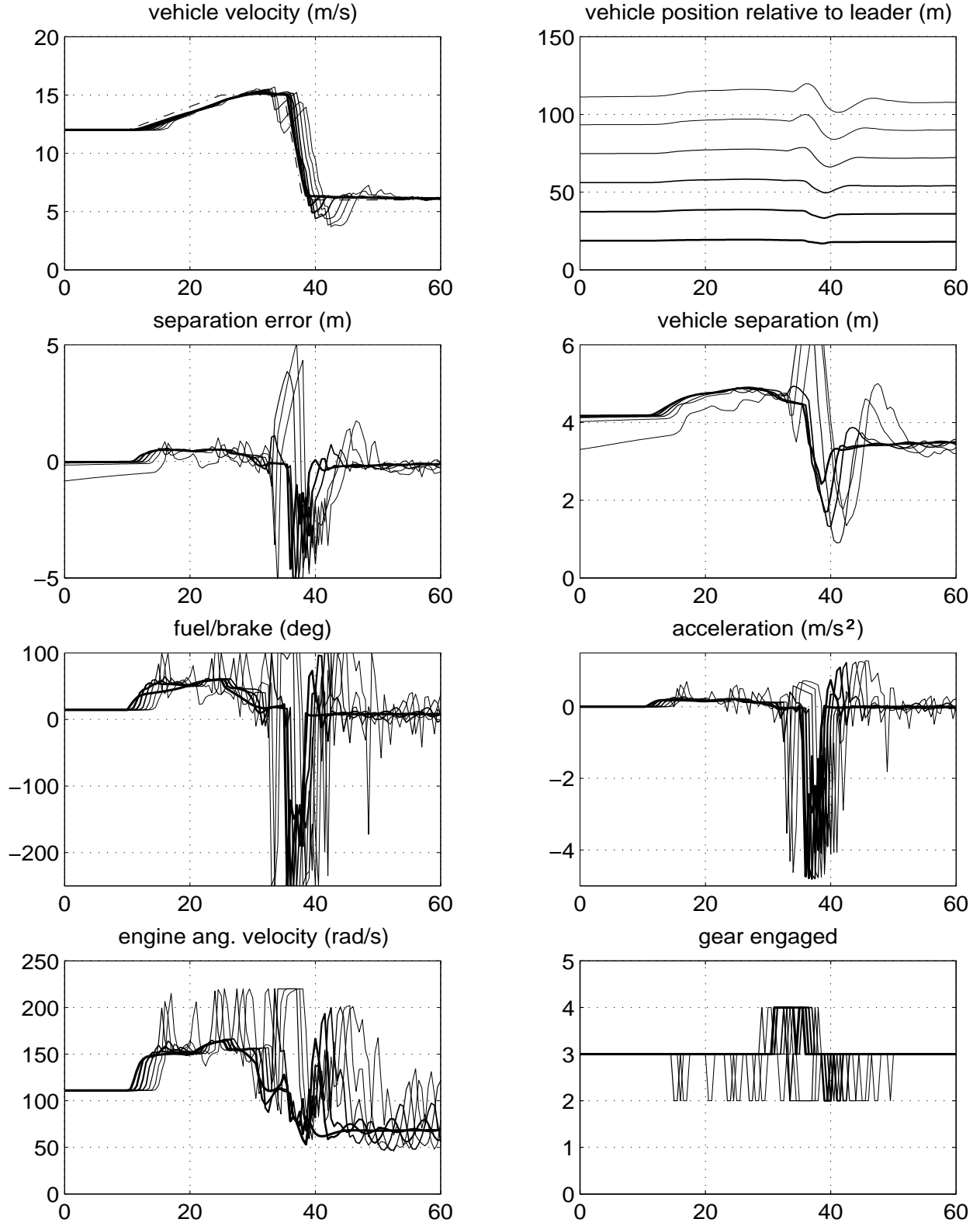
**Figure 21**: Actuator delay $\tau = 0.3$ s, backstepping controller, variable time headway $h = 0.1 - 0.2v_{\mathrm{r}}$ s, and variable separation error gain $k = 0.1 + (1 - 0.1)e^{-0.1\delta^2}$.
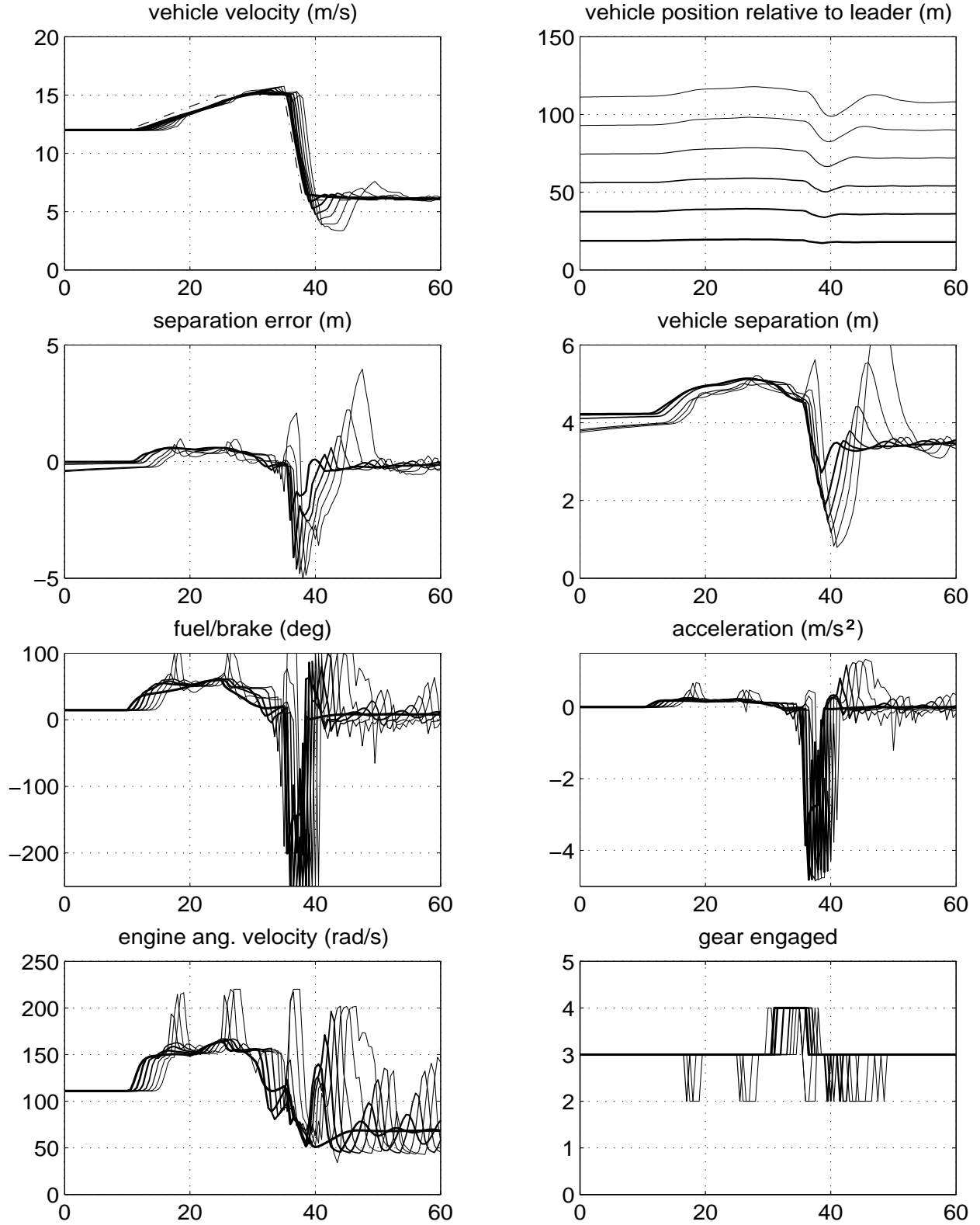
**Figure 22**: Actuator delay $\tau = 0.3$ s, backstepping controller with alternative predictor, $l = 5$, $\Delta = 0.06s$, variable time headway $h = 0.1 - 0.2v_\mathrm{r}$ s, and variable separation error gain $k = 0.1 + (1 - 0.1)e^{-0.1\delta^2}$.
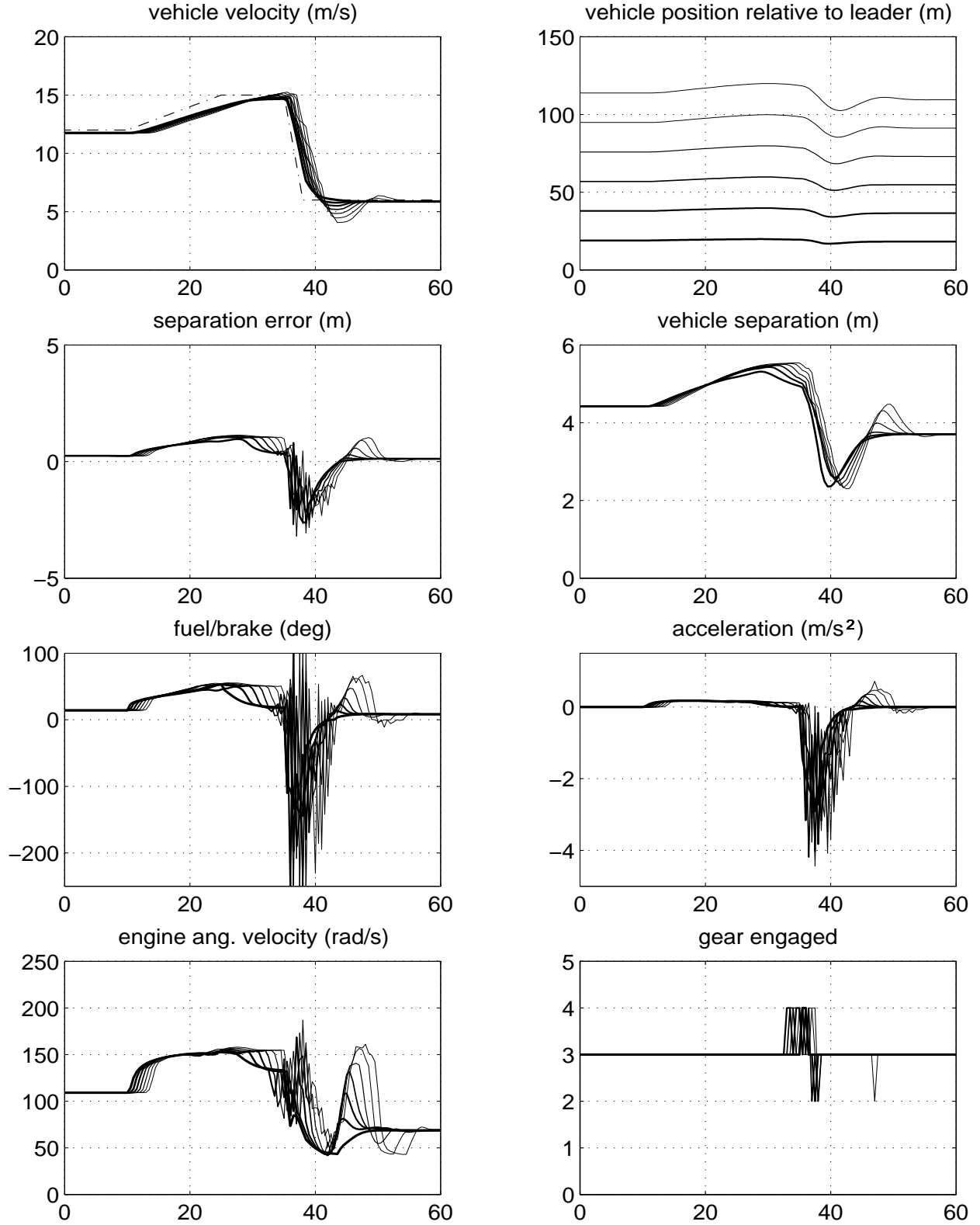
**Figure 23**: Actuator delay $\tau = 0.2$ s, PID controller, variable time headway $h = 0.1 - 0.2v_r$ s, and variable separation error gain $k = 0.1 + (1 - 0.1)e^{-0.1\delta^2}$.

32

**Figure 24**: Actuator delay $\tau = 0.2\,\mathrm{s}$, PID controller with alternative predictor, $l = 5$, $\Delta = 0.04s$, variable time headway $h = 0.1 - 0.2v_\mathrm{r}$ s, and variable separation error gain $k = 0.1 + (1 - 0.1)e^{-0.1\delta^2}$.

33

**Figure 25**: Actuator delay $\tau = 0.3$ s, PID controller, variable time headway $h = 0.1 - 0.2v_r$ s, and variable separation error gain $k = 0.1 + (1 - 0.1)e^{-0.1\delta^2}$.
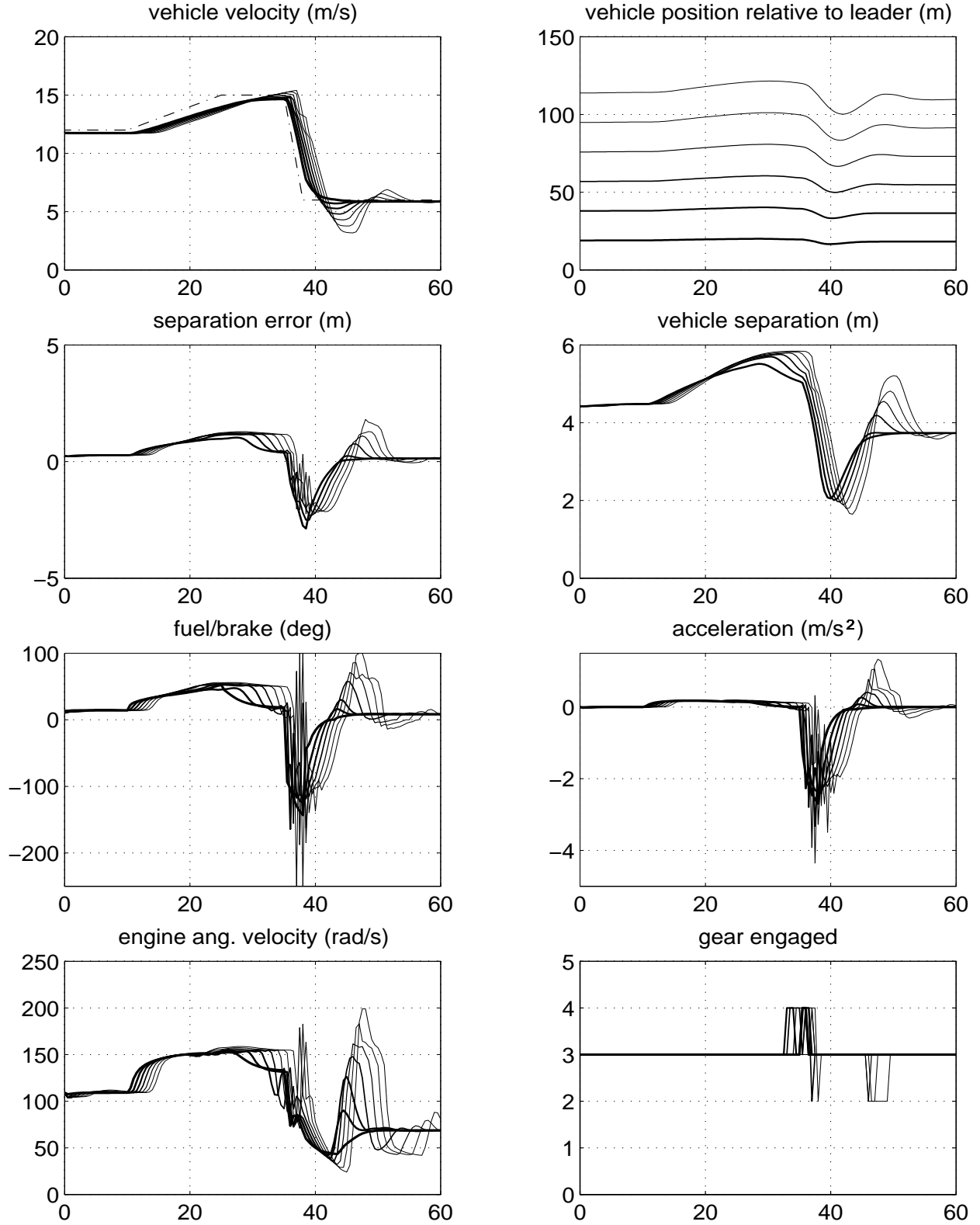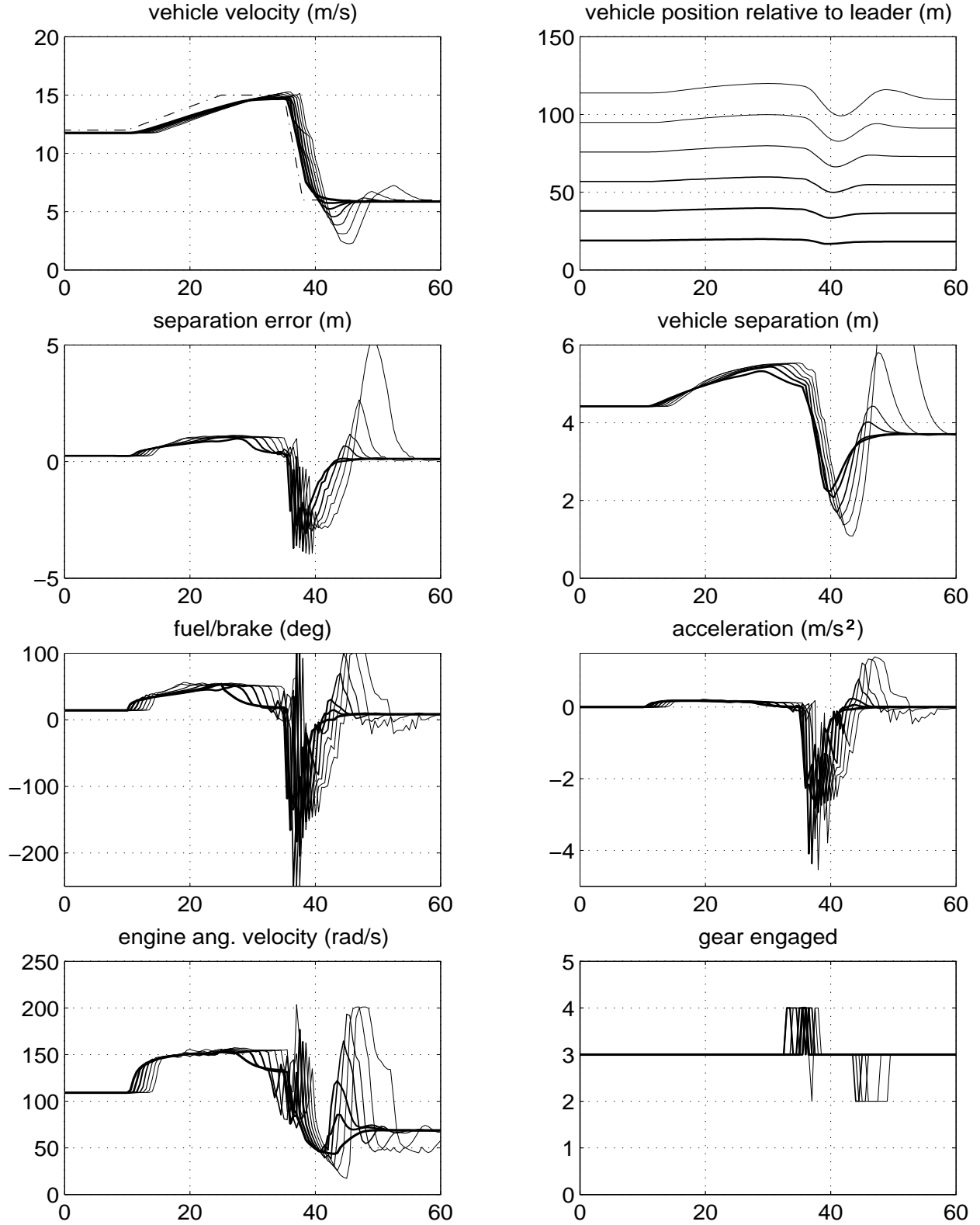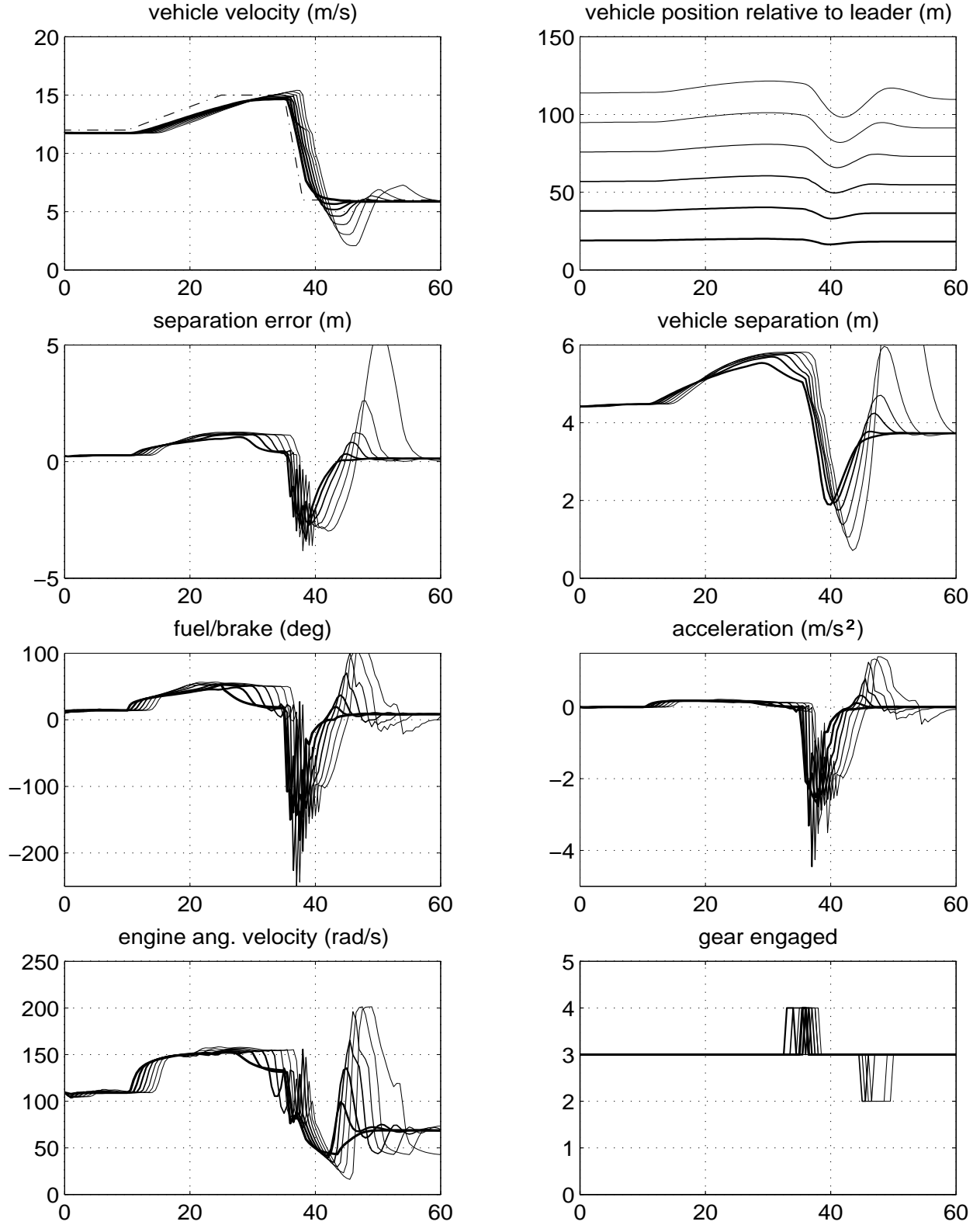
34

**Figure 26**: Actuator delay $\tau = 0.3$ s, PID controller with alternative predictor, $l = 5$, $\Delta = 0.06s$, variable time headway $h = 0.1 - 0.2v_{\mathrm{r}}$ s, and variable separation error gain $k = 0.1 + (1 - 0.1)e^{-0.1\delta^2}$.

35

# 4 Qualitative Comparison

Considering the importance of implementation cost when dealing with AHS applications, we give a graphical qualitative comparison of the new control schemes, which not only summarizes the results presented in the former sections, but also allows designers to better negotiate the trade-offs between platoon performance, control smoothness, robustness, and controller complexity in the choice of a scheme which best fits the needs of a particular implementation. First of all, we combine *robustness with respect to maneuvers* and *robustness with respect to actuator delays* into one criterion called *robustness*. This not only allows us to represent things graphically, but also gives the designer a "one-shot" picture of the available options. The robustness with respect to maneuvers is evaluated as by Yanakiev and Kanellakopoulos (1998), where two additional types of maneuvers were considered: (a) a challenging "merge" maneuver, in which two platoons of $5$ trucks each merge from an initial spacing of $83$ m to a final spacing of only $3$ m, and (b) an even more challenging "merge/brake" maneuver, in which $5$ s after the merge maneuver described in (a) has commenced, the front platoon brakes hard from $22$ m/s to $12$ m/s. Based on these simulation results we draw the 3D comparison diagram in Fig. 27.

As expected, the schemes discussed in this section offer improved platoon performance, control smoothness and, undoubtedly, are more robust with respect to actuator delays. The only thing that may seem surprising, is the worse overall robustness of schemes with predictor compared to the ones without. This is due to the fact that the schemes with predictor perform poorer in extremely challenging maneuvers as the merge/brake considered here. This makes sense intuitively: The predictor attempts to "figure out" ahead of time what is going to happen in $\tau$ s and when something totally unexpected happens, the predictor is misleading rather than helping.

Our results show that the cumulative effect of actuator delays in platoons of automated vehicles without intervehicle communication is not an insurmountable obstacle. If design simplicity, cost of implementation and computational requirements are not primary concerns, then one can nearly recover the original "delay-free" performance by using the more complex nonlinear control scheme of section 3.2 with the predictor of Fig. 10; this is seen by comparing Fig. 17 to Fig. 20. On the other hand, if simplicity and ease of implementation are more important, one can still achieve acceptable performance by using the simpler PID-based nonlinear scheme of section 3.5.

It is important to note that we do not assume perfect knowledge of the plant model; our results incorporate a great deal of modeling uncertainty due to the fact that the models we use for control design are only crude approximations of our complex simulation models. The only parameter which is assumed to be very well known is the actuator delay used in the design of our predictor. However, further simulations have indicated that the performance is not affected by small errors in this assumed value. Nevertheless, in real applications it is nearly impossible to measure this value with high accuracy, primarily because these delays change significantly with temperature and operating conditions. Hence, if the performance requirements dictate that these delays be fairly well known, it may be necessary to install torque sensors on the wheels in order to perform on-line measurements of the time it takes for a fuel or brake command to affect vehicle acceleration.
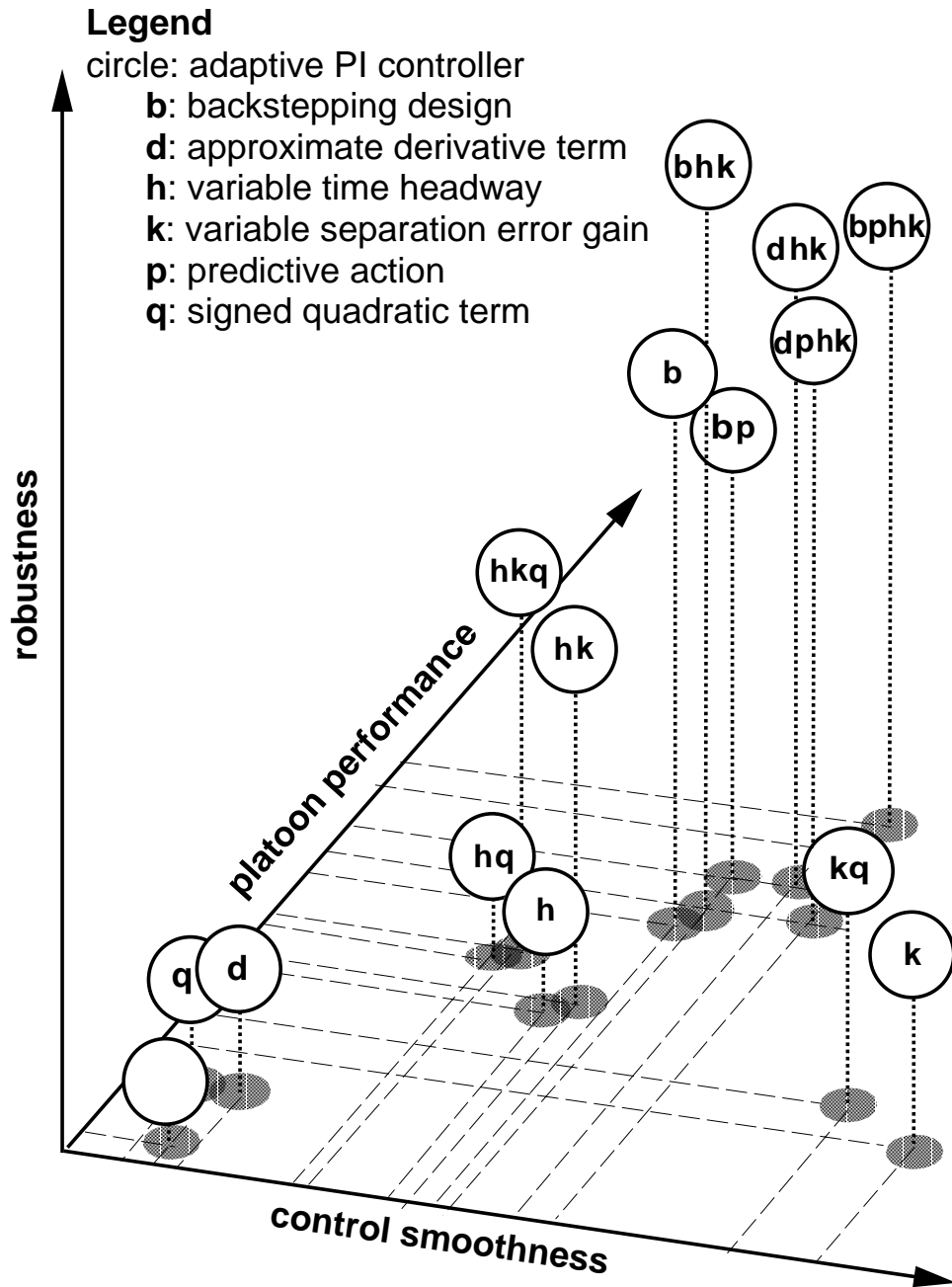
**Figure 27**: Qualitative comparison diagram.

# References

Bottiger, F., H. D. Chemnitz, J. Doorman, U. Franke, T. Zimmermann, and Z. Zomotor. 1995. Commercial vehicle and transit AHS analysis. *Precursor Systems Analyses of Automated Highway Systems*, Final Report, vol. 6, Federal Highway Administration, Report FHWA-RD-95-XXX.

Chien, C., and P. Ioannou. 1992. Automatic vehicle following. Proceedings, American Control Conference, Chicago, IL, pp. 1748–1752.

Chien, C., Y. Zhang and C. Y. Cheng. 1995. Autonomous intelligent cruise control using both front and back information for tight vehicle following maneuvers. Proceedings, American Control Conference, Seattle, WA, pp. 3091–3095.

Cho, D., and J. K. Hedrick. 1989. Automotive power train modeling for control. *Transactions of the ASME, Journal of Dynamic Systems, Measurement, and Control*, vol. 111, pp. 568–576.

Cogan, H. F. 1983. A simple method for the estimation of air brake systems actuation times. *Braking of Road Vehicles*.

Fancher, P., Z. Bareket, and G. Johnson. 1993. Predictive analyses of the performance of a highway control system for heavy commercial vehicles. Proceedings, 13th IAVSD Symposium, Supplement to *Vehicle System Dynamics,* vol. 23, pp.128–141.

Garrard, W. L., R. J. Caudill, A. L. Kornhauser, D. MacKinnon, and S. J. Brown. 1978. State-of-the-art of longitudinal control of automated guideway transit vehicles. *High Speed Ground Transportation Journal*, vol. 12, pp. 35–68.

Hedrick, J. K., D. H. McMahon, V. K. Narendran, and D. Swaroop. 1991. Longitudinal vehicle controller design for IVHS systems. Proceedings, American Control Conference, Boston, MA, pp. 3107–3112.

Heusser, R. B. 1991. Heavy truck deceleration rates as a function of brake adjustment. *SAE Transactions*, paper no. 910126.

Hurtig, J. K., S. Yurkovich, K. M. Passino, and D. Littlejohn. 1994. Torque regulation with the General Motors ABS VI electric brake system. Proceedings, American Control Conference, pp. 1210–1211.

Ioannou, P., and Z. Xu. 1994. Throttle and brake control systems for automatic vehicle following. *IVHS Journal*, vol. 1, pp. 345–377.

Krstić, M., I. Kanellakopoulos, and P. Kokotović. 1995. *Nonlinear and Adaptive Control Design*. New York, NY: Wiley Interscience.

Leasure, W. A., and S. F. Williams. 1989. Antilock systems for air-braked vehicles. *SAE Transactions*, paper no. 890113.

Ledger, J. D., R. S. Benson, and N. D. Whitehouse. 1971. Dynamic modeling of a turbocharged diesel engine. *SAE Transactions*, paper no. 710177.

McMahon, D. H., J. K. Hedrick, and S. E. Shladover. 1990. Vehicle modeling and control for automated highway system. Proceedings, American Control Conference, San Diego, CA, pp. 297–303.

Post, T., P. Fancher, and J. Bernard. 1975. Torque characteristics of commercial vehicles. *SAE Transactions*, paper no. 750210.

Radlinski, R. W., and M. A. Flick. 1986. Tractor and trailer brake system compatibility. *SAE Transactions*, paper no. 861942.

Sheikholeslam, S., and C. A. Desoer. 1990. Longitudinal control of a platoon of vehicles. Proceedings, American Control Conference, San Diego, CA, pp. 291–297.

Shladover, S. E. 1978. Longitudinal control of automated guideway transit vehicles within platoons. *Transactions of the ASME, Journal of Dynamic Systems, Measurement, and Control*, vol. 100, pp. 302–310.

Smith, O. J. M. 1957. Closer control of loops with dead time. *Chemical Engineering Progress*, vol. 53, pp. 217-219.

University of Michigan, Seminar Notes on Brakes and Brake Actuation Systems.

Varaiya, P. 1993. Smart cars on smart roads: problems of control. *IEEE Transactions on Automatic Control*, vol. 38, pp. 195–207.

Xu, Z., and P. Ioannou. 1994. Adaptive throttle control for speed tracking. *Vehicle System Dynamics*, vol. 23, pp. 293–306.

Yanakiev, D., and I. Kanellakopoulos. 1995. Variable time headway for string stability of automated heavy-duty vehicles. Proceedings, 34th IEEE Conference on Decision and Control, New Orleans, LA, pp. 4077–4081.

Yanakiev, D., and I. Kanellakopoulos. 1996. Speed tracking and vehicle follower control design for heavy-duty vehicles. *Vehicle System Dynamics*, vol. 25, pp. 251–276.

Yanakiev, D., and I. Kanellakopoulos. 1998. Nonlinear spacing policies for automated heavy-duty vehicles. *IEEE Transactions on Vehicular Technology*, vol. 47, to appear.

Yang, Y. T., and B. H. Tongue. 1996. A new control approach for platoon operations during vehicle exit/entry, *Vehicle System Dynamics*, vol. 25, pp. 305–319.